Hui *et al. Energy Mater* 2023;3:300055
DOI: 10.20517/energymater.2023.60

Energy Materials

Review

Open Access

Check for updates

Cathode materials in microbial electrosynthesis systems for carbon dioxide reduction: recent progress and perspectives

Su Hui[1,#], Yujing Jiang[1,#], Yuanfan Jiang[1], Zhaoyuan Lyu[2], Shichao Ding[3], Bing Song[4], Wenlei Zhu[1], Jun-Jie Zhu[1,*]

[1]School of Chemistry and Chemical Engineering, School of Environment, State Key Laboratory of Analytical Chemistry for Life Science, State Key Laboratory of Pollution Control and Resource Reuse, the Frontiers Science Center for Critical Earth Material Cycling, Nanjing University, Nanjing 210023, Jiangsu, China.
[2]School of Mechanical and Materials Engineering, Washington State University, Pullman, WA 99164, USA.
[3]Department of Nanoengineering, University of California San Diego, La Jolla, CA 92093, USA.
[4]Scion, Te Papa Tipu Innovation Park, Rotorua 3046, New Zealand.
[#]Authors contributed equally.

***Correspondence to:** Prof. Jun-Jie Zhu, State Key Laboratory of Analytical Chemistry for Life Science, School of Chemistry and Chemical Engineering, Nanjing University, Nanjing 210023, Jiangsu, China. E-mail: jjzhu@nju.edu.cn

How to cite this article: Hui S, Jiang Y, Jiang Y, Lyu Z, Ding S, Song B, Zhu W, Zhu JJ. Cathode materials in microbial electrosynthesis systems for carbon dioxide reduction: recent progress and perspectives. *Energy Mater* 2023;3:300055. https://dx.doi.org/10.20517/energymater.2023.60

Received: 12 Aug 2023 **First Decision:** 25 Sep 2023 **Revised:** 16 Oct 2023 **Accepted:** 26 Oct 2023 **Published:** 9 Nov 2023

Academic Editor: Yuhui Chen **Copy Editor:** Fangling Lan **Production Editor:** Fangling Lan

Abstract

Microbial electrosynthesis (MES) is an emerging technology that enables the synthesis of value-added chemicals from carbon dioxide (CO_2) or inorganic carbon compounds by coupling renewable electricity to microbial metabolism. However, MES still faces challenges in achieving high production of value-added chemicals due to the limited extracellular electron transfer efficiency at the biotic-abiotic interfaces. To overcome this bottleneck, it is crucial to develop novel cathodes and modified materials. This review systematically summarizes recent advancements in cathode materials in the field of electrocatalyst-assisted and photocatalyst-assisted MES. The effects of various material types are further investigated by comparing metal-free and metal materials and photocatalyst materials of different semiconductor types. Additionally, the review introduces the maximum production rate of value-added chemicals and conversion efficiency achieved by these cathode materials while highlighting the advantages and disadvantages of different material types. To the best of our knowledge, in electrocatalyst-assisted systems, the maximum CH_4 yield on graphene aerogel/polypyrrole cathode achieved 1,672 mmol m^{-2} d^{-1}, and the maximum Faraday efficiency (FE) of CH_4 reached up to 97.5% on graphite plate.

Meanwhile, the maximum acetate yield achieved 1,330 g m^{-2} d^{-1} with CO_2 conversion efficiency into acetate close to 100% on carbon nanotube cathodes. In photocatalyst-assisted systems, the maximum acetate yield could reach 0.51 g L^{-1} d^{-1} with the coulombic efficiency of 96% on the $MnFe_2O_4$/g-C_3N_4 photocathode. Finally, prospects for future development and practical applications of MES are discussed, offering theoretical guidance for the fabrication of cathode materials that can improve production efficiency and reduce energy input.

Keywords: Microbial electrosynthesis, cathode materials, electrochemically active microorganisms, extracellular electron transfer, photocatalyst

INTRODUCTION

With the development of the economy, the climate change resulting from greenhouse gas emissions, particularly carbon dioxide (CO_2), has become the most urgent challenge faced by human society[1]. Despite substantial efforts to curb carbon emissions and implement clean energy technologies, it is estimated that nearly 500 gigatons of CO_2 will still be released into the atmosphere by 2060 due to the combustion of fossil fuels[2]. Moreover, as fossil fuels gradually deplete, there is an urgent need to find alternatives to fossil fuels for energy and feedstocks in the production of commodity chemicals[3]. In light of emission reduction targets, the production of fuels and chemicals from CO_2 not only has the potential to mitigate global warming but also to replace traditional non-renewable fossil fuels, achieving the goal of turning waste into treasure[4].

Since the concept of microbial electrosynthesis (MES) was proposed in 2010, the field of MES has provided a completely new perspective on CO_2 reduction[5]. MES is an emerging technology that enables the synthesis of value-added chemicals from CO_2 or inorganic carbon compounds by coupling renewable electricity to microbial metabolism[5,6]. In a MES process, electrical energy is used to supply low-potential electrons to electrochemically active microorganisms (EAMs), which could reduce CO_2 in the atmosphere to fuels, including methane, ethanol, acetic acid, other short- and medium-chain fatty acids, and their corresponding alcohols[7,8]. Specifically, EAMs on the cathode utilize CO_2 as a carbon source and apply electrons as energy sources to convert inorganic carbon into value-added organic compounds through their own metabolic pathways. On the anode, water splitting reactions or other oxidation reactions take place, as shown in Scheme 1. Compared to traditional electrochemical synthesis and CO_2 reduction methods, MES allows for the production of more complex chemical compounds with higher selectivity and lower potential using abundant, renewable, and environmentally friendly EAMs found in nature[9,10]. However, MES still faces limitations in achieving high yields of value-added chemicals, falling far short of the expected levels required for competitive commercial chemical synthesis[11]. The underlying reasons for this limitation are closely related to the core of MES, namely, the acquisition of electrons by EAMs from cathodes for their own metabolism[12]. On the one hand, the insufficient conductivity and catalytic activity of cathode materials restrict the availability of direct and indirect electron donors for EAMs, leading to low extracellular electron transfer (EET) efficiency[8,13]. On the other hand, during the operation of MES reactors, only a small portion of the bacteria on the outer surface of the electroactive biofilm can make contact with the cathode material, compromising EET efficiency, biomass transport, and gas transportation[14,15]. As a result, the majority of MES systems are currently limited to laboratory scale and are not yet technologically feasible for practical production[16].

Given the aforementioned effects, the cathode and its modified materials play a crucial role in the electron transfer at the interface, the EET efficiency of EAMs, CO_2 catalysis, and the enrichment of microorganisms during MES processes. To construct an efficient cathode, ideal materials should possess specific desirable characteristics such as excellent biocompatibility, high catalytic activity, low charge transfer resistance, large

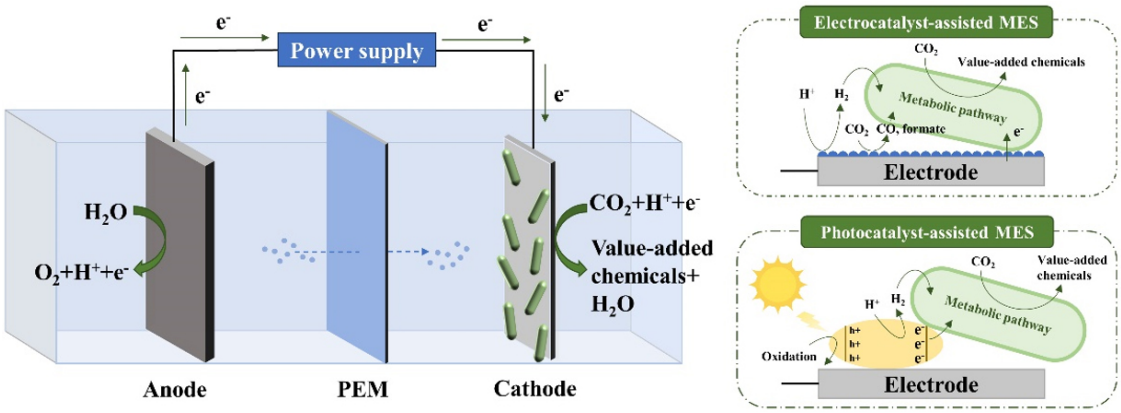

Scheme 1. Schematic diagram of a MES system for CO_2 reduction.

surface area, high durability, and low production cost[17]. In recent years, various types of novel cathode-modified materials have emerged[18]. For example, cost-effective carbonaceous materials with good biocompatibility can be utilized to form three-dimensional (3D) nanomaterials, such as carbon nanotubes (CNTs)[19] and graphene[20], which provide ample space for bacterial colonization and biomass mass transfer. Conducting polymers introduce excellent hydrophilicity and tunable electrical conductivity into the cathode, contributing to the formation of electroactive biofilms and enhancing EET efficiency[21]. Metals and their compounds exhibit extraordinary electrocatalytic activity, enabling the production of hydrogen (H_2)[22], carbon monoxide (CO)[23], formate[24], and other cathodic products that act as electronic mediators facilitating electron transport in solution. Nevertheless, existing cathode materials still fail to meet the demand for high chemical yields, primarily due to low EET efficiency, necessitating further exploration by researchers.

To overcome the aforementioned bottlenecks, it is imperative to develop more efficient cathode materials capable of reducing the overpotential of CO_2 reduction and improving the interaction between EAMs and cathode materials, thus surpassing the limitations of EET efficiency. It requires conducting a comprehensive summary of the development of cathodes since the concept of MES was proposed. This review systematically summarizes recent advancements in cathode materials within the field of electrocatalyst-assisted and photocatalyst-assisted MES. The effects of various material types are further investigated by comparing metal-free and metal materials and photocatalysts categorized according to different types of semiconductors. Furthermore, the maximum production rate of value-added chemicals and current density achieved by these cathode materials in MES systems are compared, highlighting the advantages and disadvantages of different material types. Finally, we offer prospects for future development and practical applications of MES to provide theoretical guidance for further research of cathode materials that can improve production efficiency in MES systems to reduce energy input.

CATHODE MATERIALS FOR ELECTROCATALYST-ASSISTED MES

Metal-free materials

Metals and their compounds are widely used as catalysts for industrial manufacture, clean energy generation and storage, and many other important applications. However, metal-based catalysts, particularly noble metals such as platinum, iridium, and palladium, suffer from significant drawbacks, including high cost, low selectivity, poor durability, susceptibility to gas poisoning, and negative environmental impact[25]. As a result, metal-free catalysts, such as carbon-based materials and conducting polymers, have emerged as promising alternatives to platinum catalysts, offering enhanced efficiency at a

lower cost in many fields[26,27]. This section presents a comprehensive overview of metal-free catalysts in MES cathodes, specifically focusing on carbon-based materials and conductive polymers, which have been utilized as modifications to enhance cathode performance. The profound impact of metal-free catalysts on the overall performance of MES is thoroughly discussed, taking into account their contributions to EET, microbial colonization, and gas mass transfer.

Carbonaceous materials

Carbonaceous materials have gained significant preference as electrode materials in various applications due to their diverse morphologies, remarkable chemical stability, and high specific surface area[28]. Particularly, an increasing number of carbon materials are derived from sustainable biomass precursors, such as coconut shells, mango seed husks, and grape marcs, making carbonaceous materials more environmentally friendly and cost-effective[29,30]. Moreover, the outstanding biocompatibility and conductivity of carbonaceous materials play a crucial role in promoting the proliferation of electroactive bacteria and facilitating EET. These advantages have been widely applied in microbial electrochemical systems, such as microbial fuel cells (MFC)[31,32] and microbial electrolysis cells (MEC)[33,34]. Similarly, carbon-based electrodes were among the earliest materials employed in MES systems, primarily due to their ability to provide a stable immobilization matrix for electroactive biofilms[5,35]. Due to the swift advancements in nanomaterials, a notable disparity arises in terms of conductivity, specific surface area, and electrocatalytic activity between conventional carbonaceous materials and their innovative counterparts[36,37]. Therefore, it becomes crucial to modify or develop advanced carbonaceous electrodes with superior structures or higher catalytic activity to improve the performance of MES. For example, carbonaceous materials with high specific surface area, such as granular activated carbon (GAC) and carbon nanoparticles (CNPs), could increase the contact between electrode materials and EAMs to enhance EET efficiency. Carbonaceous materials with 3D structures, such as carbon felt (CF) and graphite felt (GF), can provide sufficient colonization space for EAMs. Nano carbonaceous materials, represented by CNTs and graphene, are being widely investigated in various fields due to their excellent properties, such as high conductivity and catalytic activity. This section highlights the key findings and implications of utilizing advanced carbonaceous electrodes for CO_2 conversion via MES.

Due to the dependence of the core of MES on EET from the cathode to EAMs, improving the biotic-abiotic interface can enhance the performance of these systems. Compared to a conventional graphite rod electrode, the utilization of graphite granules in the cathode chamber promotes better contact between EAMs and cathode materials, resulting in enhanced electron uptake efficiency. In long-term operations of MES reactors, graphite granule cathodes with acetogenic bacteria inoculated achieved an acetate production rate of 1.04 g L^{-1} d^{-1} at a poised potential of -0.59 V (*vs.* standard hydrogen electrode, SHE)[38]. However, the irregular shape of carbon particles and the porosity of the cathode chamber bed can contribute to higher electrical resistance in MES systems and the potential for biomass clogging[39]. To address these challenges, fluidized bed reactors incorporating a functional cathode with GAC have been developed. These reactors offer a simplified construction, efficient particle mixing, prevention of biomass blockage, and improved contact efficiency between particles and substrates. Consequently, they exhibit enhanced electroactivity and provide ample space for substrate transportation[40]. Furthermore, researchers have explored the use of nitrogen-modified carbon materials to enhance the durability of the cathode[41]. Nitric acid-treated graphite particles with nitrogen elements introduced exhibited enhanced electron transfer performance, serving as cathode materials for more efficient CO_2 reduction[42]. In this study, the MES system utilizing nitric acid-treated graphite particles as the cathode yielded 1.4 times more acetate compared to the system using untreated graphite particles[42].

To improve electron transfer at the cathode interface, it is necessary to enhance the conductivity and electrocatalytic activity of cathode materials while reducing the activation energy of electron transfer. Over the past few decades, graphene and its derivatives, such as graphene oxide (GO) and reduced GO (rGO), have been used to modify cathodes in MES systems, leading to significant advancements in chemical production owing to their excellent electrical conductivity, remarkably high carrier mobility, superior chemical stability, outstanding specific surface area, and biocompatibility[43,44]. To realize economic production in practical applications, intermittent gas supply can help maximize the utilization of gas by microorganisms, but it will cause deterioration of the bio-methanation process[45,46]. Due to the high electrical conductivity and large surface specific area of graphene, the cathode could stabilize bio-methanation after experiencing intermittent gas supply, with the gas conversion efficiency and CH_4 production rate increased by 18.2% and 267%, respectively, as compared with the control[20]. Nevertheless, the application of graphene is hindered by its low dispersibility and tendency to aggregate in aqueous environments[47]. As the most common derivative of graphene, GO is further incorporated with a large amount of oxygen-containing functional groups to enhance the interface interaction inside graphene, such as hydroxy and epoxide groups, thereby improving the stability of electrodes[48]. At the same time, there are abundant cymbal and carboxyl groups on the edges of GO, which determine its superior hydrophilicity and facilitate the adhesion and electron transfer of EAMs[49,50]. In the case of rGO, it introduces more structural defects to achieve higher electrocatalytic activity while retaining residual oxygen and other miscellaneous atoms[51]. An *in situ* self-assembled rGO/biofilm system, in which rGO was reduced by EAMs, was constructed for highly efficient acetate production for the first time[52]. The addition of a substantial amount of rGO in the biofilm has significantly enhanced the EET efficiency, thereby achieving an increase of 1.5 times the acetate production rate in MES systems[52]. If rGO was functionalized with tetraethylene pentamine (TEPA) to obtain positive charges, the self-assembled rGO-TEPA-modified carbon cloth (CC) cathode with spatial arrangement could tensely arrange with *Sporomusa ovata* (*S. ovata*) with negative charges[53]. With the dense and robust electroactive biofilm forming, the acetate production rate was increased by 3.6 times[53].

On the other hand, the electroactive biofilms formed through simple adsorption typically exhibit low levels of colonization on the hydrophobic low-dimensional carbon electrodes, which is another factor constraining the efficiency and performance of MES systems frequently. Therefore, in order to allow more biomass adhesion, the cathode surface should be functionalized to increase hydrophily[54]. According to this, the functional group modification of chitosan, cyanuric chloride, and 3-aminopropyltriethoxysilane on CC led to the enhancement of positive charge and increased the formation rate of acetate[55]. Another strategy to enhance biomass is to expand the specific surface area of cathodes to gain more bacterial colonization space, so it is imperative to develop high-performance 3D electrodes. Reticular vitreous carbon (RVC) is an amorphous carbonaceous material with spatial reticular structures, which is often used as a substrate electrode in electroanalytical chemistry[56]. However, unmodified RVC electrodes are not suitable for MES due to the lack of nanostructures to develop biofilms. To address this issue, flexible multiwalled CNTs were directly grown on RVC to create a novel type of biocompatible and highly conductive 3D cathode (NanoWeb-RVC), allowing for enhanced bacterial attachment and biofilm development within its hierarchical porous structure[19]. Compared to the carbon plate control group, 1.7 and 2.6 folds higher current density and acetate production rate were reached on NanoWeb-RVC cathodes[19]. By electrophoretic deposition, a more uniform and homogeneous layer of CNTs can be grown on the honeycomb structure of RVC [Figure 1A, B, D, and E]. The high surface specific area introduced by nanostructures can maximally enable the biocatalyst loading and allow the formation of continuous electroactive biofilms with faster EET [Figure 1C and F][57]. On this novel biocathode, the current density and acetate productivity reached -200 A m^{-2} and 1,330 g m^{-2} d^{-1} severally, with electrons and CO_2 recoveries into acetate of mature biofilms being very close to 100% [Figure 1G-I][57]. This is the highest performance output we have ever investigated up to now.

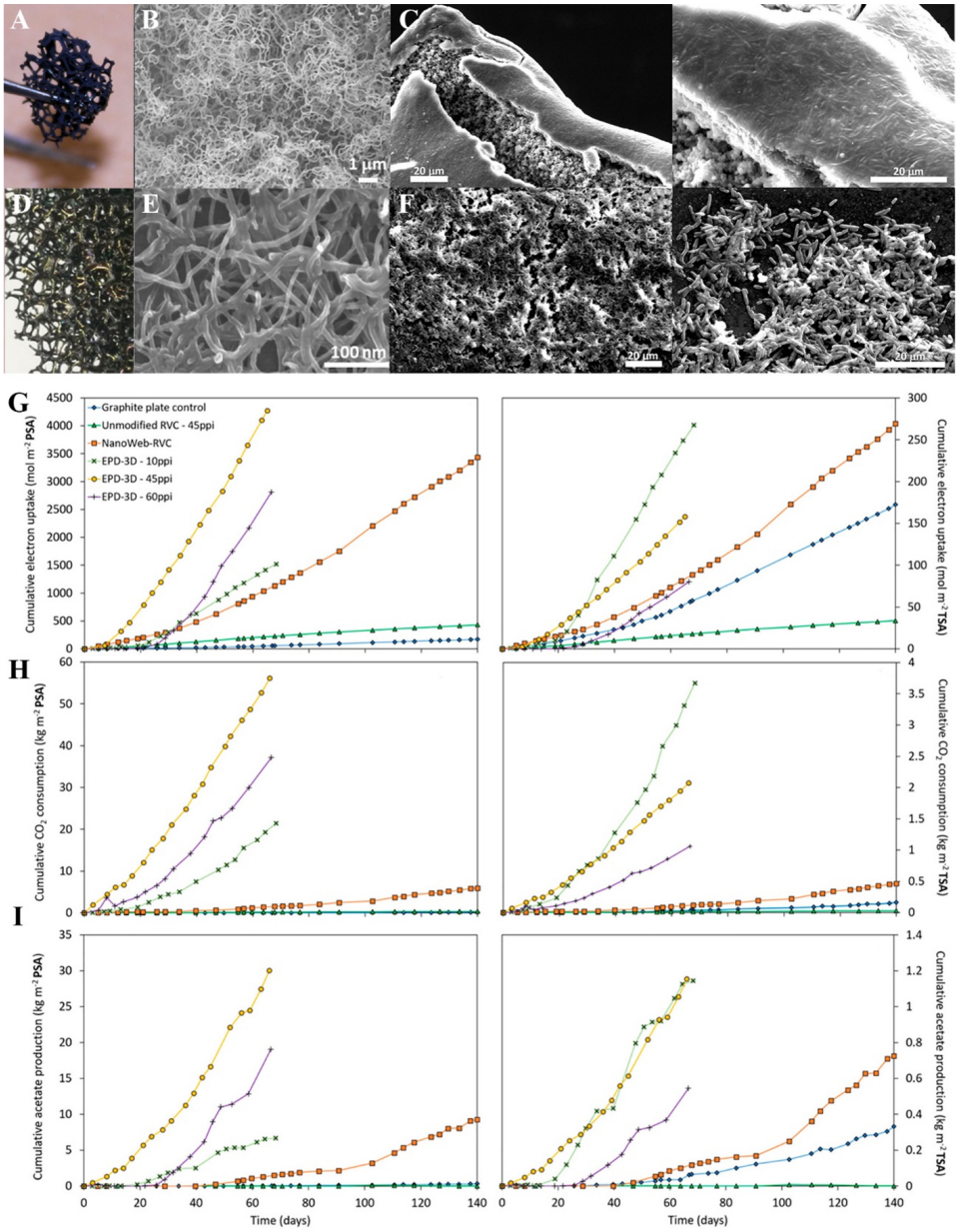

Figure 1. (A) Photographic images and (B) Scanning electron microscopy (SEM) micrographs for NanoWeb-RVC. (C) SEM micrographs of putative electroactive biofilms grown on NanoWeb-RVC after 140 days of inoculation. (D) Photographic images and (E) SEM micrographs for EPD-3D. (F) SEM micrographs of putative electroactive biofilms grown on EPD-3D 45 ppi after 63 days of inoculation. (G) Cumulative electron consumption, (H) CO_2 consumption, and (I) acetate production over time on graphite plate, unmodified RVC 45 ppi, NanoWeb-RVC 45 ppi, and EPD-3D 10 ppi, 45 ppi, and 60 ppi, normalized to projected surface area (left) and total surface area (right). This figure is quoted with permission from Flexer *et al.*[57].

Moreover, carbon brush, as a conductive material with a high specific surface area, has the advantage of less bacterial clogging possibility and faster mass transfer because of its open brush structure compared with other carbonaceous braided materials[58]. The yield of CH_4 and the proportion of CO_2 reduction in the MES reactor with carbon brush were much higher than those with the graphite plate[59]. Next, the effect of surface area on the current generation and anaerobic digestion performance was investigated by adding carbon brush electrodes of different sizes. Adding a high surface area carbon fiber brush is a more effective method

for improving anaerobic digestion performance[60]. CF, with interlaced carbon fibers to construct open 3D spatial structures, is another excellent cathode material owing to its low cost, high surface area, and good biocompatibility[61]. Based on these characteristics, CF cathodes could provide sufficient space and suitable environments for the formation of electroactive biofilms. In contrast to the GAC electrode, CF biocathodes in MES systems showed a higher CH_4 production rate of 2,840 ± 450 mL L^{-1} d^{-1} and acetate production rate of 1.42 ± 0.22 g L^{-1} d^{-1} at a continuous CO_2 flow[62]. Electrochemical experiments have confirmed that MES systems could enable CO_2 consumption maximum by forming efficient electroactive biofilms on the 3D structure of CF, leading to significantly enhancing acetic acid production[63]. The CH_4 yield and coulomb efficiency (CE) can also be improved by modifying GF layers on ordinary carbon rods as a biocathode[64]. In addition to the biomass attached to the cathode, the initiation rate of electroactive biofilms is also crucial for the industrial application of MES systems. The biofilm formed by placing GF directly in the anaerobic reactor possessed high electroactivity and strong direct electron transfer ability[65]. The start-up time was shortened by at least 20 days, and the charge transfer resistance was reduced by 4.45-10.78 times in comparison to the common start-up method of inoculating cathode effluent or granular sludge into the cathode chamber. Nevertheless, the bare CF still suffered from the aforementioned problem of poor electrochemical activity, and the modified CF could enhance the cathode-organic interaction to solve this bottleneck. A novel Prussian blue nanocube-modified CF (PBNCs-CF) as an artificial electron mediator-decorated cathode was designed, with enhanced acetate production reaching 0.20 ± 0.01 g L^{-1} d^{-1} in MES systems[66]. The biocompatibility of CF cathodes was increased by the unique hydrophilicity and positive charge of PBNCs, which was in favor of the growth of biofilms on the cathodic surface and internal fibers[66]. Meanwhile, owing to the rapid electronic transition between Fe^{2+} to Fe^{3+} ions, PBNCs significantly improved the electrochemical activity of the CF cathode by increasing the electron supply to EAMs dramatically. Graphene nanosheets with an amorphous shape are also coated on the scaffold to further enlarge the surface specific area of the cathode and introduce high electrocatalytic activity. CF cathodes coated with 3D graphene were fabricated by a solvothermal synthesis process for more efficient electron transfer in MES inoculated with *S. ovata*[67]. The 3D structure improved biofilm density significantly to increase the acetate production rate by 6.8 times[67]. According to the same thought, the effect of graphene as cathode materials on organics production, such as acetate and butyrate, was evaluated, with the current density increasing by 85.7% and the total electron recovery reaching the MES system by more than 90%[68]. Furthermore, in a MES system for methanogenic archaea, the current density, charge transfer resistance, and *Methanobacterium* biomass attached to CF cathodes modified with rGO were all improved[69].

Notably, some studies have reported that the microbial EET efficiency at the biological interface inside the biofilm is much lower than that at the biotic-abiotic interface[12]. Since most of the materials or catalysts were modified on the base electrode surface, only the bacteria in the inner layer of the biofilm could make direct contact with conductive materials. Nanomaterials may enhance EET efficiency by forming hybrid biofilms with bacteria to participate in long-distance electron transfer inside cathodes. The utilization of carbon nanomaterials to mix bacteria on the anode has been demonstrated to effectively enhance the enrichment of the exoelectrogens and facilitate anodic electricity generation[70]. In accordance with this concept, a biohybrid membrane was formed by co-precipitating *Moorella thermoacetica* and CNPs on the CC cathode[71]. Compared with the native biofilm, the addition of CNPs to the biofilm resulted in a significant improvement in the yield of acetate and formate to 2.68 and 3.80 g m^{-2} d^{-1} by representing an increase of 14 and 7.9 times, respectively, which was the highest yield reported on two-dimensional (2D) electrodes[71]. The large specific surface area of CNPs might provide more effective sites for bacterial colonization and electron uptake, enhancing the physical contact of bacteria to the electrodes.

In addition to the EET efficiency, another bottleneck in the MES process is the hindered mass transfer of CO_2 gas in the cathodic chamber and on conventional cathodes. Hollow fiber membranes (HFMs), which enable direct gas permeation from the inside of the membrane filaments, can address this issue. The utilization of HFMs ensures that CO_2 can be efficiently used by the electroactive biofilm, minimizing gas wastage[72]. Consequently, HFMs were modified on the CF to enhance CO_2 mass transfer while increasing the electrical conductivity of the cathode simultaneously[73]. This strategy of supplying CO_2 within the electrode presents a novel concept for regulating the microenvironment of MES systems.

Conducting polymer

Nevertheless, the hydrophobicity of carbonaceous materials inhibits the release of gas and the infiltration of water, which not only adversely affects the mass transfer of CO_2 but also greatly reduces the likelihood of microbial attachment. To address these challenges, the inherent characteristics of conducting polymers, such as adjustable electrical conductivity, electrochemical stability, exceptional hydrophilicity, and high biocompatibility, align more closely with the requirements for constructing cathodes in MES systems[74]. Conductive acrylonitrile butadiene styrene polymer rods were assembled to form a 3D cathode, which increased both acetate and CH_4 production by promoting biofilm development[62]. As the limitation of the specific surface area of rod-shaped electrodes gradually emerges, the development of novel nanostructured conductive polymer cathode materials becomes an active topic. By means of the electrospinning technique, polyaniline (PANI) is fabricated as a 3D scaffold with high surface volume ratios, significant fiber interconnectivity, and microscopic porosity[55]. The acetate production rate on PANI cathodes was three times higher than for the control CC cathode, with a recovery of electrons consumed in acetate production of 85% ± 7%. Whereas the cost is taken into account, based on the 3D carbonaceous electrode to promote biomass and gas transport, modifying additional conductive polymer materials to enhance microbial adhesion and direct EET is a more typical strategy. By electropolymerizing conductive poly (3,4-ethylenedioxythiophene) (PEDOT) onto the GO film, a novel GO/PEDOT cathode was fabricated, with a maximum CH_4 production rate of 315.3 ± 13.2 mmol m^{-2} d^{-1} and a high FE of 92%[75]. There is no doubt that the GO/PEDOT film not only enhanced the microbial colonization by the crosslinked fibers but also improved the biofilm formation. As previously reported, 3D materials are typically synthesized through hydrothermal[76] and chemical reduction[77] methods, while the 3D structure often exhibits poor controllability and repeatability due to the difficulty of tuning the nanosheet assembly by these conventional methods[78]. Recently, 3D printing technology has been recognized as a promising way to construct hierarchical porous structures that excel in the preparation of regular and periodic open channels to improve biomass transport and microbial colonization of 3D electrodes[79]. A 3D-printed graphene aerogel (GA)/polypyrrole (PPy) cathode with hierarchical porous structures was prepared with the CH_4 production rate reaching 1,672 ± 131 mmol m^{-2} d^{-1}, which was higher than that of the cathodes prepared by conventional methods [Figure 2A, B, and F][21]. The high CH_4 yield was on account of the fact that PPy coating improved the interface interaction between the biofilm and the cathode, exhibiting low mass transfer resistance and a relatively dense biofilm [Figure 2C, D, and E].

The primary approach to enhance the performance of MES has been focused on improving H_2-based electron uptake by reducing overpotential and increasing electrode electrical conductivity. However, electrode-based direct electron uptake is theoretically more efficient[80]. To achieve this, a solid neutral red/Nafion conductive layer was introduced on the surface of a carbonaceous electrode, enhancing its redox capability and hydrophobicity[81]. The cathode with the solid neutral red/Nafion conductive layer exhibited higher carbon and electron recovery efficiency for CO_2 conversion, resulting in a two-fold increase in acetate production rate compared to the unmodified carbonaceous electrode[81]. To enhance direct EET of EAMs, another strategy of single-bacterial surface modification opened new avenues recently, which built

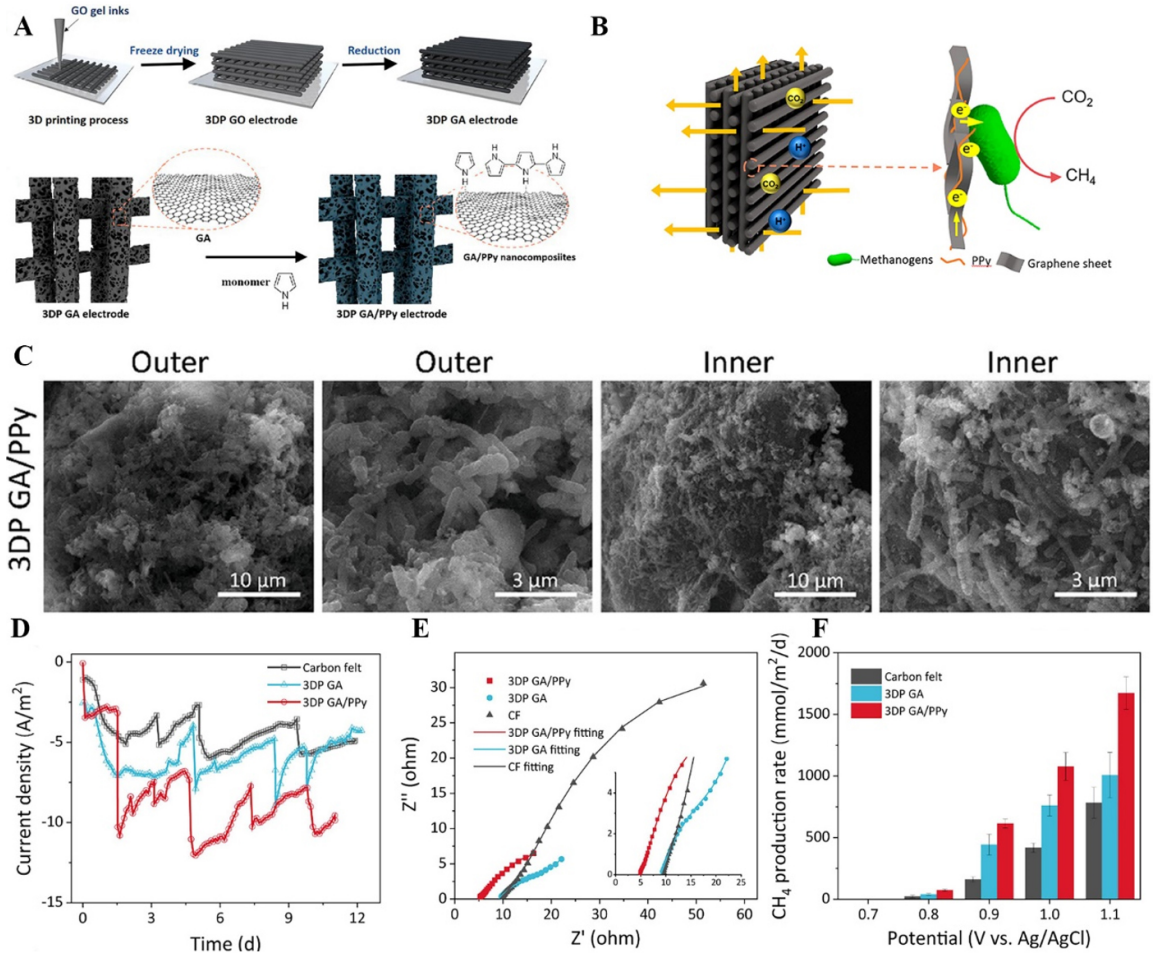

Figure 2. (A) Schematic diagram of 3DP GA electrode preparation (up) and polymerization of the 3DP GA/PPy electrode (down). (B) Schematic diagram of the 3DP GA biocathodes facilitating ion and gas transport. (C) SEM images of biofilm formation on the 3DP GA/PPy cathodes from the outer and inner electrode surface. (D) Start-up current of the biocathodes at the potential of -1.0 V *vs.* Ag/AgCl. (E) EIS curves. (F) CH_4 production rate of the 3DP GA and CF biocathodes. This figure is quoted with permission from He *et al.*[21].

an interconnected conductive layer on and across the individual bacterial membrane *in situ*[82]. The high conductive PPy was coated on the surface of acetogenic bacteria, and the PPy-coated bacteria were inoculated on the cathode of MES, leading to a 33%-70% decreased charge transfer resistance and 3-6 times increased acetate production rate of PPy-coated biocathodes[83]. Although PPy-coated biocathodes with lower resistance achieved higher current density, acetate production rate, and FE compared to uncoated biocathodes, the low level of C-type cytochrome expression on biocathodes suggested that the inwards EET pathway may be different from the bioanode in MFC. Therefore, further studies are needed to investigate the electron transfer mechanism of EAMs on the cathode of MES.

When using gaseous CO_2 as the carbon source, considering that the biological reduction process depends on the dissolution and mass transfer of CO_2 in the electrolyte, the gas diffusion electrode (GDE) combined with the conducting polymer membranes has received extensive attention in the field of MES. GDEs are porous electrodes that support electrocatalysts, whereas conducting polymer membranes are polymeric materials that conduct ions between electrodes, which both affect the chemical environment and performance of the electrolyzer[84]. A combination of the porous activated carbon and Teflon binder as the

catalyst layer and the hydrophobic gas diffusion layer created a three-phase interface at the electrode, which could facilitate CO_2 and reducing equivalents to be available to the biocatalyst on the cathode surface[85]. At the same time, more commercialized GDEs have been developed to better suit amplifying MES systems. Three-chamber electrochemical cells equipped with GDEs evolved an efficient cathodic community dominated by *Acetobacterium* that achieved CO_2 conversion to acetate with the highest production rate of 55.4 g m^{-2} d^{-1}, with exceeding CE of 80%[86]. Compared to traditional immersed electrodes, GDEs have potential effectiveness in facilitating faster delivery of gaseous CO_2 and also provide adsorption of CO_2 to electrochemical active sites, leading to higher expected productivity when equipping GDEs in MES.

Metal materials

Although significant progress has been made in the research and modification of metal-free materials, they still fall short in terms of matching the stability and electrical conductivity of biocathodes in MES. Metal materials, known for their excellent electrical conductivity, stability, and superior catalytic activity, have been widely recognized as effective electrode modification materials in microbial electrochemical systems[87]. Noble metals, such as Ir, Pt, and Pd, have demonstrated excellent electrocatalytic activity but are limited by their high cost and low abundance[88,89]. Therefore, the search for efficient non-precious metal catalysts for practical applications is crucial. Non-noble monometallic catalysts, including manganese (Mn), iron (Fe), cobalt (Co), nickel (Ni), and copper (Cu), have received significant attention due to their ability to reduce CO_2 to electronic mediators, such as H_2 and formate, which can be utilized by electroactive bacteria. In this section, particular emphasis will be placed on monometallic materials, alloys, and inorganic metal compounds, especially those that facilitate the catalysis of indirect electron mediators.

Monometallic catalysts

Monometallic catalysts possess desirable controllable properties and are relatively easy to prepare, making them attractive as catalysts and materials for cathode modification. Electrical-biological hybrid cathodes were fabricated using electrocatalyst foils from four different metal groups: indium (In), zinc (Zn), titanium (Ti), and Cu[90]. Constant current electrochemical experiments revealed that the four metal electrodes exhibited high parallelism at the current density of 30 A m^{-2}, while only the maximum acetic acid production rate (1.23 ± 0.02 g L^{-1} d^{-1}, 313 ± 5 g m^{-2} d^{-1}) of the Zn-based electrode was further increased when the current density increased to 50 A m^{-2}[90]. From the comparison of these four metal materials, Zn-based electrodes were certified as more conducive to CO_2 valorization by bacteria at a high current density. Ni and Fe, on the other hand, seem to have advantages in increasing CH_4 production owing to their availability, high conductivity, and low cost. By introducing $NiSO_4$ or $FeSO_4$ into the cathode electrolyte, Ni and Fe were deposited *in situ* on the CF, respectively, with the current density and CH_4 production significantly improving[91]. In the previous studies on the electrocatalytic reduction of CO_2, Cu has been commonly recognized as the only metal capable of catalyzing the formation of multi-carbon (C_{2+}) from CO_2 because of its unique d-band center[92-94]. Even though Cu has been replaced in MES by biocatalysts with better selectivity, it is still favored because of its high conductivity and low H_2 evolution properties. Especially the substrates produced from Cu catalysts, such as formate, ethanol, and methanol, can be utilized by certain methanogens. Cu-based electrodes with several different structures and preparation technologies were compared to the performance of MES-containing graphite block cathodes, and all Cu-based cathodes showed better methane production, except for the copper foil, which lacked a biocompatible surface[95]. Among them, the preparation technologies of copper electrodes, for instance, electroless and electro-deposited, have the greatest impact on the bioelectrochemical performance of MES systems.

Relative to bulk materials, metal nanoparticles (NPs) with excellent catalytic activity, biocompatibility, high active surface area, and chemical stability have been widely used for enhancing electron exchange[96]. Most of all, the size of the metal NPs can be easily adjusted to match the size of the electroactive bacteria. Inspired

by metal anodes in MFCs, thin layers of gold (Au), palladium (Pd), or Ni NPs were homogeneously coated onto the CC by physical deposition, and each of the treatments for Au, Pd, and Ni promoted acetate production rates with 6, 4.7, or 4.5 folds faster than the untreated control, respectively[55]. Considering the cost of precious metals, non-precious metal NPs were further introduced into MES. The presence of molybdenum (Mo) NPs had no significant effect on the acetate production but increased the CH_4 production, while Ni and Cu NPs lengthened the lag period of acetate production, which demonstrated that metal NPs largely affected the relative abundance and metabolism of EAMs[97].

In the liquid-phase environment of MES systems, the conventional approach for delivering CO_2 to the chemoautotrophs on the cathode is by bubbling gaseous CO_2. However, due to the low solubility of gaseous CO_2 in the solution, diffusion and mass transfer limitations may arise, thereby impacting the conversion and efficiency of MES[98]. As previously mentioned, bubble-less gas exchange HFMs have been utilized as cathode structures to facilitate a three-phase interface involving CO_2 gas, cathodic biofilms, and electrolytes, which configuration enables efficient gas transfer and mass transport, enhancing the overall performance of the system[99,100]. The novel-designed cathode consisted of porous nickel hollow fibers and hydrogenotrophic methanogens, which act as an inorganic electrocatalyst for H_2 generation from proton reduction and a biological catalyst reducing equivalents for the conversion of CO_2 to CH_4, respectively [Figure 3A, D, and E][22]. In order to further improve the formation of biofilms and the product generation rate on the cathode, nanomaterials were modified on the nickel hollow fiber cathode to enlarge the specific surface area and enhance electron transfer between electrodes and microorganisms. Remarkably, the porous nickel hollow fibers modified with CNTs resulted in a 76.3% reduction of cathode electron transfer resistance [Figure 3B] and a significant 11-fold increase in the CO_2 adsorption capability at atmospheric pressure [Figure 3C], contributing to the higher acetate production rate of 1.85 ± 0.13 g m^{-2} d^{-1} in MES inoculated *S. ovata* [Figure 3F][101]. However, on account of the high fabrication cost of nickel, the utilization of ceramic hollow fiber (CHF) membranes as substrate electrodes might be a more affordable option. By one-step electroless plating nickel on CHF, the multifunctional cathode can enrich chemoautotrophs mainly composed of *S. ovata* on the surface of membrane cathodes and reach an acetate production rate of as high as 71.72 ± 4.33 g m^{-2} d^{-1}[102]. Apart from the improved CO_2 mass transfer efficiency inherent on the CHF, the microfiltration function provided by the membrane structure can simultaneously achieve a high acetate recovery of more than 87.1%[102]. The effect of CO_2 flow fluctuations on the stability of MES systems can also be further explored on CHF. CHF wrapped with Ni-foam/CNTs electrode sparged CO_2 directly to EAMs, significantly increasing biochemical yields with a higher CE of 51.5%, which laid a foundation for the practical application of MES[103]. It could be concluded from the above research that the hybrid approach of combining electrolysis with bioconversion presented a novel pathway for generating highly diverse long-chain valuable chemical products with higher efficiency.

In addition to nickel as an electrocatalyst to produce H_2, syngas (CO/H_2) can also be used as a gaseous feedstock and electron mediator for microbial utilization, which allows faster electron transfer than direct contact, which may be rate-limited[104]. Previous research has shown that silver (Ag), as a common metal catalyst for electrocatalytic reduction to produce CO, could produce syngas from the CO_2 electrolyzer, which was coupled with a fermentation module to convert CO_2 to butanol and hexanol with high carbon selectivity[105]. For better tunable electrochemical syngas production, a porous Ag GDE was fabricated on the CNT-supported hydrophobic membrane, with aCO faradic efficiency of approximately 92% and larger tunable CO/H_2 ratios in the optimized reactor[23]. This study brought possibilities for integrating electrochemical and biological processes to enable CO_2 reduction and chain elongation of chemicals. Following a similar two-step integrating strategy, formate reduced from CO_2 can also be utilized as the organic substrate and electron mediator for the growth of many kinds of microorganisms[106]. The tin (Sn)

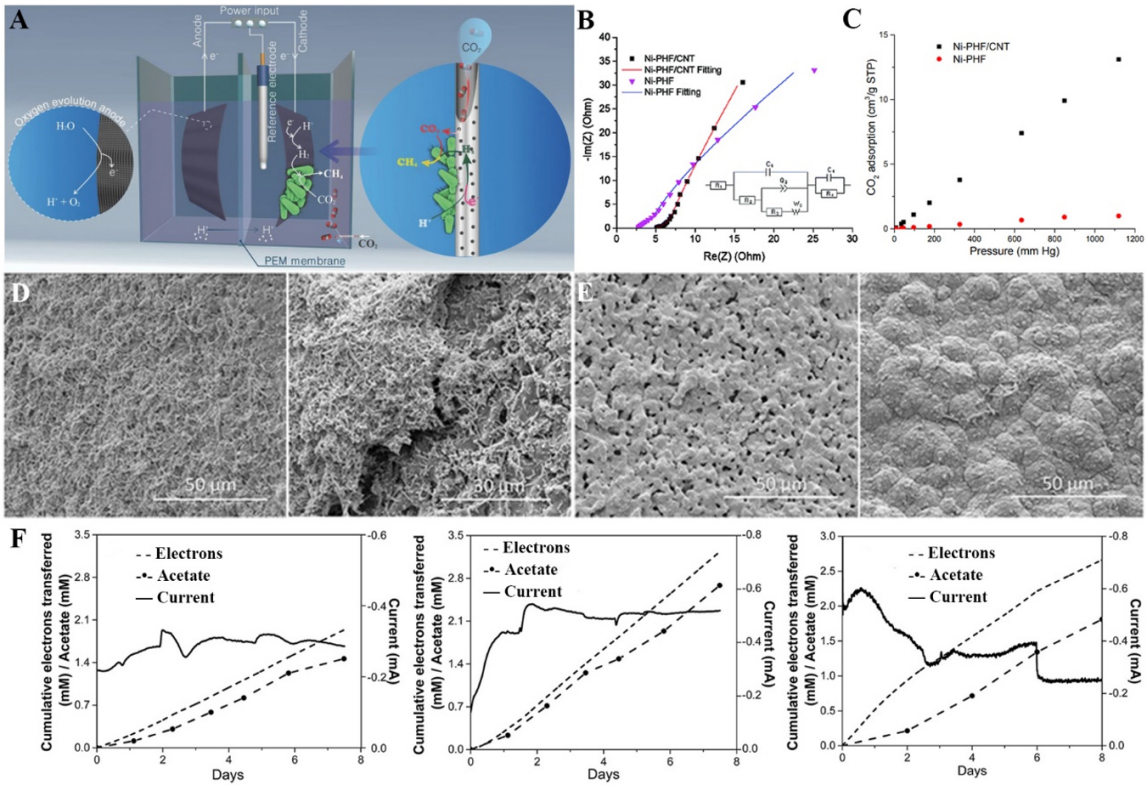

Figure 3. (A) A schematic of a MES reactor showing the replacement of a conventional submerged flat cathode with an electrically conductive, catalytic, and porous hollow-fiber (CCPHF) cathode. (B) Nyquist plots of Ni-PHF and Ni-PHF/CNT in sterile blank medium. The inset is the equivalent circuit for EIS fitting. (C) Comparison of CO_2 adsorption capability of Ni-PHF and Ni-PHF/CNT cathodes. SEM images taken at the end of batch 8 for the cathodic biofilms developed on (D) Ni-CCPHF cathodes of an experimental reactor and (E) Ni-CCPHF that was used only as a gas-transfer membrane for CO_2 delivery (left) and served only as a cathode (right). (F) Electron transfer, measured acetate production, and current consumption of the Ni-PHF cathode (left) and the Ni-PHF/CNT cathode (middle), both with direct CO_2 delivery through the pores of the hollow fibers. MES performance of the Ni PHF/CNT cathode (right) with CO_2 bubbled into the medium. This figure is quoted with permission from Alqahtani *et al.*[22] and Bian *et al.*[101].

cathode reduced CO_2 to formate, and then formate, separated by electrodialysis, was consumed by methanogens to obtain CH_4[107]. Similarly, formic acids can be exploited by acetogens. Sn-modified CF was prepared by electrodeposition, with the presence of Sn accelerating the indirect electron transfer rate between EAMs and electrodes, thus improving the yield of acetate[24].

Alloys and inorganic metal compound catalysts

Compared to pure metals, alloy and inorganic metal compound catalysts exhibit distinct advantages in terms of superior performance and low cost, leading to their increasing prominence in recent years. Oxides are typically among the most stable forms of metal compounds found in nature and can be easily synthesized[108]. Ferrocene was subjected to microwave pyrolysis using CF as a microwave absorber, resulting in the growth of Fe(III) oxide-graphitized carbon on the CF electrode. This composite material exhibited a multi-length scale porous structure, offering a high specific surface area, excellent conductivity, and stability. The acetate productivity achieved was more than 1.49×10^4 g m^{-3} d^{-1}, together with an electron recovery rate of 86% ± 9%[109]. Metal oxides containing multiple metallic elements could usually combine the superiorities of different metals. Nickel ferrite ($NiFe_2O_4$) with mixed valent ions [Ni(II)/Ni(III), and Fe(II)/Fe(III)] was coated on CF, which realized improved product selectivity and enhanced butyrate production of 1.2 times in comparison to bare CF[110]. The presence of $NiFe_2O_4$ in MES cathodes achieved production of carboxylates with higher economic value and selectivity on account of the advantages of

improved electrical conductivity, charge transfer efficiency, microbial-electrode interactions, and most importantly, the selective microbial enrichment of *Proteobacteria* and *Thermotogae* (butyrate-producing phyla). Copper ferrite consists of a unique valance configuration with a high theoretical capacity and excellent electrochemical properties, which can be easily tuned by their structure and morphology with suitable synthesis methods remarkably, so it seems to show a better character of application than $NiFe_2O_4$[111]. Copper ferrite/rGO nanocomposites synthesized by the biocombustion method from citrus fruit extract exhibited a porous network-like structure and a low charge transfer resistance, thus promoting the isobutyrate and acetate production of 35.37 g m^{-2} d^{-1}[112]. There is no doubt that the method of preparing low-cost metal oxide nanomaterial cathodes from natural materials is receiving great attention.

In addition to metal oxides, 2D transition metal carbides, nitrides, and carbonitrides, such as titanium carbide ($Ti_3C_2T_X$), also known as MXenes, have gained significant attention in the past decade[113]. Owing to the abundance of surface terminations and free electrons in transition metal carbides or nitrides, MXenes possess a unique combination of hydrophilicity and metallic conductivity, which greatly facilitates the attachment of microorganisms and EET by microorganisms[114,115]. Moreover, MXenes offer an adjustable structure and rich surface chemistry, making them an excellent choice for fabricating high-performance electrodes[116]. A novel MXene-coated CF electrode was prepared and investigated for application in MES, with the formation of a continuous electroactive biofilm, and exhibited excellent current generation, resulting in a 1.6-, 1.1-, and 1.7-fold increase in the concentration of acetic, butyric, and propionic acid, respectively, compared to uncoated CF [Figure 4][117]. If MXenes were ulteriorly introduced into macroporous scaffolded CNTs by a facile dip drying method, the uniform 3D structure and abundant active sites of the coated material facilitated mass diffusion and microbial growth[118].

As widely recognized, EAMs have the capability to directly utilize electrons from the cathode or indirectly through H_2 produced by the catalyst, enabling the production of value-added chemicals from CO_2[119]. However, when an electroactive biofilm forms on the cathode, direct electron transfer is often hindered by the low conductivity of the microorganisms themselves, making electron transfer mediated by H_2 more suitable for practical applications[120]. Consequently, the integration of the H_2 evolution reaction (HER) catalyzed by inorganic electrocatalysts and the H_2-driven catalytic reaction facilitated by biocatalysts for CO_2 reduction represents a promising technology with exceptional selectivity and stability. Although precious platinum group metals are recognized as highly efficient HER electrocatalysts, their widespread deployment on a large scale is hindered by their high cost. In this regard, transition metal carbides have emerged as promising alternatives for combining with EAMs due to their remarkable catalytic activity, electrochemical stability, and cost-effectiveness[121,122]. The molybdenum carbide (Mo_2C) modified electrode was constructed as an active HER electrocatalyst, with the volumetric acetate production reaching 0.19 ± 0.02 g L^{-1} d^{-1}, which was 2-fold of the control[123]. The presence of Mo_2C accelerated the release of H_2 and regulated the mixed microbial community to promote the growth of biofilm, thus improving the CO_2 reduction rate in MES systems. In addition to metal carbide, the contribution of metal phosphide, sulfide, and alloys as catalysts for HER in MES was further investigated. Cobalt-phosphide (CoP), molybdenum-disulfide (MoS_2), and nickel-molybdenum alloy (NiMo) cathodes performed sustained H_2 evolution under conditions suitable for the growth of electroautotrophic microorganisms, achieving nearly 100% CE in an integrated system inoculated with methanogens and acetogens[124]. If the structure of inorganic metal compounds is ameliorated, the performance of MES can also be affected. MoS_2 nanoflowers were modified on the CF via a simple one-step hydrothermal method, with the HER activity higher than that of bare CF, which showed the highest volumetric acetate production rate of 0.2 g L^{-1} d^{-1} at the preparation temperatures of 180 °C[125]. The improved efficiency of MES contributed to the fact that the porous nanoflower structure of MoS_2 facilitated microbial colonization and increased the indirect and direct electron transfer efficiency.

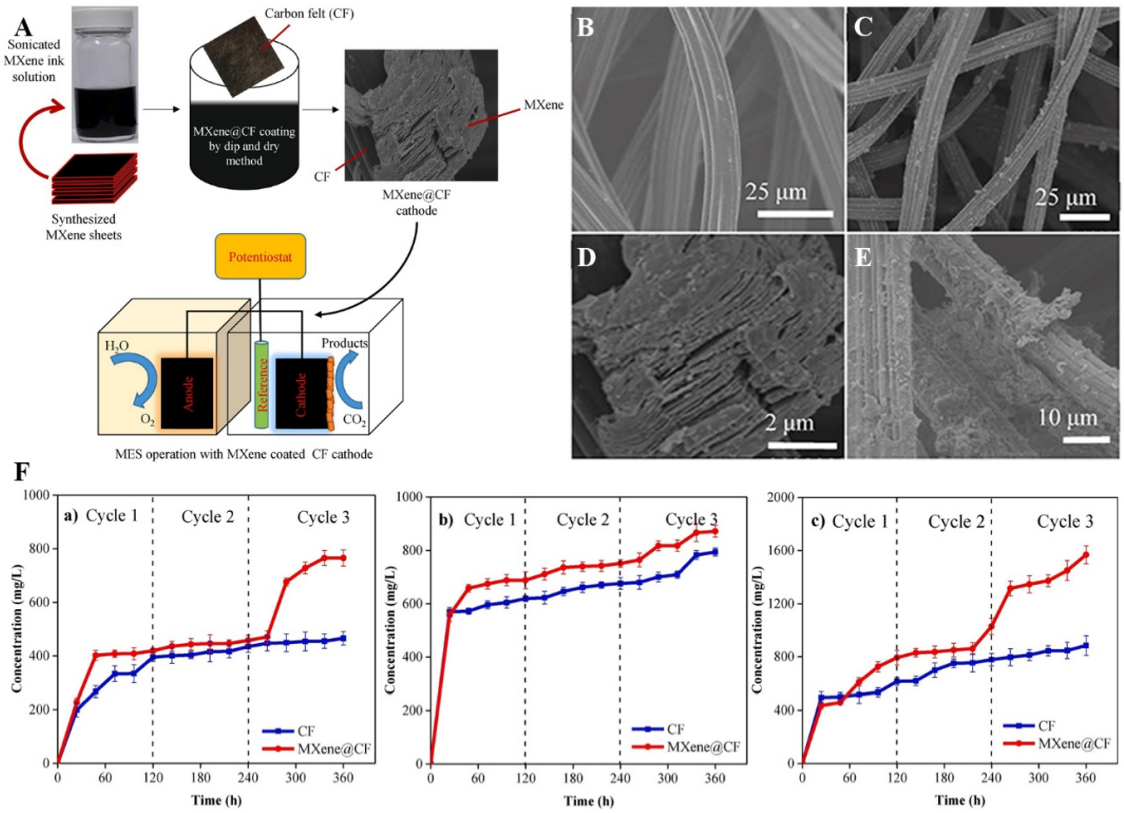

Figure 4. (A) A schematic diagram of MXene@CF electrode preparation and MES operation. SEM images of (B) plain CF, (C and D) MXene@CF, and (E) MXene@CF biofilm. (F) Accumulated concentration profile for the MES products acetic acid, butyric acid, and propionic acid (from left to right) for a MES system operated at a fixed cathode potential of -0.8 V using plain and MXene-coated CF. This figure is quoted with permission from Tahir *et al.*[117].

Despite the extensive study of H_2 as an electron donor, recent research has demonstrated that syngas serves as a more favorable electron donor for converting CO_2 into value-added chemicals due to its higher thermodynamic reducing power[105]. To capitalize on this, highly selective cobalt phthalocyanine catalysts were incorporated into MES cathodes to facilitate the production of syngas instead of H_2, resulting in enhanced bioconversion rates of CO_2 into acetate and ethanol[126]. In contrast, a 3D porous functionalized carbon electrode coated with a Co catalyst exhibited a lower applied operating potential and more stable CO production compared to a 2D planar electrode. This improvement can be attributed to the larger specific surface area provided by the CF, enabling better gas transfer through bubble formation and adhesion. Consequently, the 3D porous cathode yielded higher maximum titers of acetate (5.1 *vs.* 3.8 g L^{-1}) and ethanol (1.2 *vs.* 0.9 g L^{-1}) compared to the 2D planar cathode[126].

Composite materials

The incorporation of composite materials offers an efficient approach to enhance the performance and broaden the application range of cathodes in MES by combining the large specific surface area and hydrophilicity of metal-free materials with the high conductivity and catalytic activity of metallic materials. For example, by modifying the metal electrode with chitosan, the electrochemical performance and stability of the cathode can be significantly improved[127]. Among these composites, those composed of metallic materials and 3D carbon materials have garnered significant attention in MFCs due to their ability to provide high catalytic activity, efficient extracellular electron transport, and ample space to enhance the colonization of EAMs[128]. However, certain metals, such as Cu, are limited in bioelectrochemical systems

due to their antimicrobial properties. To address this, the introduction of rGO with high biocompatibility effectively enhances the antibacterial activity of copper foam. Consequently, this promotes the formation of a dense and electroactive biofilm of *S. ovata* on the electrode surface, leading to increased acetate yields[129].

It is noteworthy that metals not only serve as highly conductive materials to facilitate electron transport but also act as inorganic catalysts to promote the generation of H_2 and other electronic mediators in the cathode. Stainless steels, as a kind of lower H_2 evolution overpotential material, were in an assembly with GF as cathodes, producing acetate at the maximum rate of 1.3 and 2.4 mM d^{-1} in mixed culture and *Clostridium ljungdahlii* MES reactors, severally[130]. The combination of CC-stainless steel electrodes could improve the yield of volatile fatty acids (VFA) to 1.4 g L^{-1}, and the reduction current was significantly higher than the control group, which were owing to a relatively higher tendency towards reductive capabilities with lower electron losses of hybrid biocathodes[131]. With the introduction of a cost-effective packed-fluidized cathode consisting of stainless steels and GAC, pre-acclimatized GACs with active anaerobic microbes on its surface were packed in stainless steels, and CO_2 was directly flushed on the GAC surface through a pipe to ensure its availability to the biocatalyst[132]. The acetate volumetric production rate achieved 0.16 g L^{-1} d^{-1}. In addition, despite the fact that the formation of electroactive biofilms is important for electron capture, excessively thick biofilms have been demonstrated to possess an obvious influence on efficient electrochemical reactions and mass transfer, especially in MES systems with gaseous environments. Inspired by alveolus-like structures to enable gas diffusion, a hybrid electrode coupling porous hollow stainless steels with graphene foam was herein proposed for CH_4-production MES[133]. The 3D layered graphene foam structure with interconnected pores ensured the entrance of microorganisms for colonization, while the porous hollow stainless steel supplied and diffused CO_2 into the microstructure of combined graphene foam, thus achieving a high CH_4 production rate of 848.0 ± 124.5 mmol m^{-2} d^{-1}[133]. If the metals and carbonaceous materials are hybridized together, they can own better biological affinity and stability and also good electrochemical performance. A nano-titanium carburizing electrode with a nanotube array porous structure was used to increase the adsorption and utilization capacity of the polar plates for H_2 [134].

On the other hand, the inclusion of metal oxides brings about more functions to MES cathodes. Magnetite (Fe_3O_4) with oxidized Fe(III), as a natural terminal electron acceptor, can help to improve EET with advantages of good biocompatibility and low toxicity[135]. In order to avoid the drawback of aggregation of Fe_3O_4 particles owing to the nanoscale and magnetic effects, the Fe_3O_4 particles were grown on the carbon support GAC as a cathode in MES to improve the electrode conductivity and biofilm activity effectively[136]. As magnetic metal oxides, Fe_3O_4 NPs allow the fast capture of EAMs onto the magnetic substrate electrode by the magnetic activity as well. This potential has captured tremendous attention. With the magnetic attraction formed between the biological complex and the electrode by incorporating Fe_3O_4 NPs into the GO solution in advance and wrapping the magnet in a CC, a thicker hybrid mature biofilm was formed[137]. As a result, the biocathode achieved a high CH_4 production rate of 605 ± 119 mmol m^{-2} d^{-1} with a FE of 91% ± 14%. Considering that inefficient electron transfer at the interface between the biohybrid and the cathode materials is a limiting factor, a novel inorganic biological hybrid was proposed by feeding highly conductive N-doped Fe_3O_4 with carbon dot shells (Fe_3O_4@CDs) in *Geobacter sulfurreducens* to facilitate EET and energy conversion[138]. The maximum current of Fe_3O_4@CDs-fed bacteria was 6.37 times higher than that of the control group without NP addition, which was the result of the interaction network between Fe_3O_4@CDs and conductive proteins inside and outside the sulfur-reduced *G. sulfurreducens*.

More nanohybrid catalysts can be prepared by adjusting the element composition and nanoform of metal oxides. For instance, a cathode made of nanowires interconnected with flower-like morphology of MnO_2 decorated over rGO was developed for MES to produce acetate and isobutyric acids, with large surface area,

high pseudocapacitance, increased CO_2 absorption capacity, and reduced electron transfer resistance compared to bare CC[139]. The composites of the morphology of nanomaterials and advanced architectures of substrate electrodes further open new avenues for MES cathodes. Highly conductive tungsten oxide (WO_3)/rGO nanofibrous-modified CC cathodes were fabricated for increased acetate production in MES, which was 41% higher than the unmodified electrode[140]. WO_3 nanofibers helped to reduce the resistance to flow the electron and improve the electrical charge holding capacity by enhancing capacitance, while rGO supported enough space to ensure adhesion of bacterial community.

Based on the aforementioned research, it can be concluded that carbonaceous materials remain the most prevalent choice for modified cathode materials in MES due to their favorable attributes of low cost, excellent mechanical properties, and diverse morphologies. Concurrently, the advancement of nanomaterials has led to the utilization of various 3D carbon nanomaterials with high conductivity as MES cathodes, resulting in improved EET efficiency and microbial colonization. The incorporation of conductive polymers further enhances the hydrophilicity and biocompatibility of modified MES cathodes, rendering them more suitable for the growth of electroactive microbial biofilms. Furthermore, the introduction of metal materials not only enhances the cathode conductivity but also facilitates the generation of electron mediators, leveraging their notable electrocatalytic activity to enhance indirect electron transfer. Consequently, composite materials combining metal-free and metal materials have emerged as the primary focus of research for MES cathodes. The specific data of MES systems mentioned in this section are summarized in Table 1 below. By a comprehensive comparison of the data listed in Table 1, we believe that the novel 3D nano carbon cathodes could achieve the highest acetate yield of 1,330 g m^{-2} d^{-1} due to its ability to load more electroactive bacteria and exhibit higher electrochemical activity. While conducting polymer cathodes have improved tunability and hydrophilicity, which can achieve higher methane production rates, metal electrodes generally obtain higher current densities because of their superior conductivity.

CATHODE MATERIALS FOR PHOTOCATALYST-ASSISTED MES

The electrocatalyst-assisted MES system has the capability to enhance CO_2 reduction through the self-metabolism of EAMs under electrical stimulation. In contrast, the photocatalyst-assisted MES system harnesses a continuous source of solar energy from nature, offering a more sustainable and environmentally friendly solution. This system converts CO_2 into multicarbon products under solar-driven conditions, effectively reducing electricity consumption. While photosynthesis was once exclusively known as "the guarded secret of plants", humans have successfully developed the photochemical process to convert CO_2 into valuable organic products[141]. This process is now known as artificial photosynthesis, encompassing various technologies such as photocatalysis, photovoltaic-driven electrolysis, and photoelectrochemical reactions[142]. Photocatalyst-assisted MES represents an efficient photoelectrochemical reactor that combines multiple functions with low energy consumption, high CO_2 conversion efficiency, and strong electricity generation capabilities[143]. This section focuses on analyzing two types of photocatalysts: single photocatalysts and heterojunction photocatalysts, aiming to optimize cathode materials in photocatalyst-assisted MES systems.

Single photocatalyst

Typically, photosynthesis in plants is accomplished through light reactions and dark reactions. Specifically, the light reaction captures solar energy and generates the reducing agents: adenosine triphosphate (ATP) and nicotinamide adenine dinucleotide phosphate (NADPH). Subsequently, the dark reaction utilizes these reducing agents to reduce CO_2 through the Calvin cycle[143]. In the context of MES, photoelectrocatalytic cathodes capture light and provide reducing agents, typically H_2 or electrons, which serve a function similar to ATP and NADPH in the light reaction[144]. Biological catalysts then utilize H_2 or electrons to convert CO_2

Table 1. Performance of different types of cathode materials in electrocatalyst-MES systems

Cathode materials	Type of products	Microbial inoculum	Production rate	CE or FE (%)	Cathode potential (*vs.* SHE)	Current density	Ref.
Carbonaceous materials							
Graphite granules	Acetate	Enriched mixed culture (*Acetobacterium* spp. dominated)	0.2 g L^{-1} d^{-1}	84.3 ± 7.6	-0.59 V	-2.5 A m^{-2}	[38]
GAC	Acetate	Enriched mixed culture	0.16 g L^{-1} d^{-1}	62.4-73.7	-0.82 V	-1.7 A m^{-2}	[40]
Nitric acid-treated graphite granular	Acetate	Enriched mixed culture	0.17 g L^{-1} d^{-1}	65.5	-0.82 V	-5.12 A m^{-2}	[42]
Graphene	CH_4	Enriched methanogens (*Methanothermobacter* dominated)	453.6 mL d^{-1}	/	/	/	[20]
rGO	Acetate	Enriched mixed culture	0.17 g L^{-1} d^{-1}	77	-0.82 V	-4.9 A m^{-2}	[52]
rGO-TEPA	Acetate	*S. ovata* wild type	0.054 g L^{-1} d^{-1}	83 ± 4	-0.69 V	-0.19 ± 0.1 A m^{-2}	[53]
		S. ovata strain met	0.17 g L^{-1} d^{-1}	83 ± 3		-2.36 ± 1.1 A m^{-2}	
CC	Acetate	*S. ovata*	1.80 ± 0.42 g m^{-2} d^{-1}	76 ± 14	-0.37 V	-0.071 ± 0.011 A m^{-2}	[55]
CC modified with chitosan			13.75 ± 3.36 g m^{-2} d^{-1}	86 ± 12		-0.47 ± 0.018 A m^{-2}	
CC modified with cyanuric chloride			12.31 ± 3.00 g m^{-2} d^{-1}	81 ± 16		-0.45 ± 0.079 A m^{-2}	
CC modified with 3-aminopropyltriethoxysilane			5.70 ± 1.20 g m^{-2} d^{-1}	82 ± 11		-0.21 ± 0.011 A m^{-2}	
CNT-cotton			6.13 ± 1.50 g m^{-2} d^{-1}	83 ± 10		-0.22 ± 0.001 A m^{-2}	
CNT-polyester			5.76 ± 1.44 g m^{-2} d^{-1}	82 ± 8		-0.21 ± 0.013 A m^{-2}	
CNTs on RVC	Acetate	Enriched mixed culture	780.68 g m^{-2} d^{-1}	77 ± 10	-0.85 V	-37 A m^{-2}	[19]
CNTs on RVC by chemical vapor deposition	Acetate	Enriched mixed culture	192 g m^{-2} d^{-1}	70	-0.85 V	-37 A m^{-2}	[57]
CNTs on RVC by electrophoretic deposition			685 g m^{-2} d^{-1}	100	-0.85 V	-102 A m^{-2}	
			1,330 g m^{-2} d^{-1}	100	-1.10 V	-200 A m^{-2}	
Carbon brush	CH_4	Enriched mixed culture	5.2 mmol d^{-1}	18.8	-0.50 V	-4.07 × 10^{-4} A m^{-2}	[59]
Graphite plate			4.3 mmol d^{-1}	97.5		-6.63 × 10^{-5} A m^{-2}	
Carbon brush	CH_4	Enriched mixed culture	59 ± 17 mL d-1	3.4	-0.80 V	2.7 A m^{-3}	[60]
CF	CH_4	Enriched mixed culture	2,840 ± 450 mL L^{-1} d^{-1}	95	-2.80 V	-190 ± 14 mA	[62]
	Acetate		1.42 ± 0.22 g L^{-1} d^{-1}				
GAC	CH_4		1,420 ± 188 mL L^{-1} d^{-1}	80-95		-184 ± 18 mA	
	Acetate		0.47 ± 0.13 g L^{-1} d^{-1}				
CF	Acetate	Enriched mixed culture	2.20 g L^{-1}	53	-0.68 V	/	[63]
GF	CH_4	Enrich the methanogens	80.9 mL L^{-1} d^{-1}	194.4	-1.40 V	/	[64]
GF	CH_4	Enrich the methanogens	29.00 mL L^{-1} d^{-1}	113.7	-0.80 V	/	[65]
PBNC-CF	Acetate	Enriched mixed culture	0.20 ± 0.01 g L^{-1} d^{-1}	63	-0.85 V	-4.5 A m^{-2}	[66]

3D graphene functionalized CF	Acetate	*S. ovata*	0.12 ± 0.04 g L^{-1} d^{-1}	86.5 ± 3.2	-0.69 V	-2.45 ± 0.16 A m^{-2}	[67]
Graphene-modified CF	Acetate	Enriched mixed culture	262 mg L^{-1}	95.1	-0.57 V	-2.6 ± 0.1 A m^{-2}	[68]
	Butyrate		84.8 mg L^{-1}				
rGO-CF	CH_4	Enrich the methanogens	/	/	-0.77 V	-1.2 A m^{-2}	[69]
CNPs on CC	Acetate	*M. thermoautotrophica*	3.49 g m^{-2} d^{-1}	65	-0.40 V	-0.063 A m^{-2}	[71]
	formate		2.91 g m^{-2} d^{-1}				
Conducting polymer							
CC modified with PANI	Acetate	*S. ovata*	5.40 ± 1.32 g m^{-2} d^{-1}	85 ± 7	-0.37 V	-0.19 ± 0.018 A m^{-2}	[55]
Conductive acrylonitrile butadiene styrene polymer	CH_4	Enriched mixed culture	500 ± 70 mL L^{-1} d^{-1}	89 ± 12	-2.80 V	-185 ± 13 mA	[62]
	Acetate		2.21 ± 0.26 g L^{-1} d^{-1}				
GO/PEDOT	CH_4	Enriched mixed culture	315.3 ± 13.2 mmol m^{-2} d^{-1}	92	-0.67 V	-2.54 A m^{-2}	[75]
3D-printed GA/PPy aerogel	CH_4	Enrich the methanogens	1,672 ± 131 mmol m^{-2} d^{-1}	85.3	-1.10 V	-23.74 A m^{-2}	[21]
Solid neutral red/Nafion conductive layer	Acetate	Enriched mixed culture	1.60 g L^{-1} d^{-1}	74	-0.77 V	-0.1 A m^{-2}	[81]
PPy-coated	Acetate	The acetogens	21.27 ± 2.82 mg L^{-1} d^{-1}	6.0 ± 2.1	-0.33 V	-56.4 ± 7.6 A m^{-3}	[83]
Porous activated carbon and Teflon binder with gas diffusion layer	Acetate	Enriched mixed culture	238 mg L^{-1} d^{-1}	72.5	-0.90 V	-20 A m^{-2}	[85]
VITO-Core® GDE	Acetate	Enriched mixed culture	55.4 g m^{-2} d^{-1}	80	-0.84 V	-10 A m^{-2}	[86]
Monometallic catalysts							
Zn	Acetate	Enriched mixed culture	1.23 ± 0.02 g m-^{2} d^{-1}	~100	-0.87 V	-50 A m^{-2}	[90]
			313 ± 5 g m^{-2} d^{-1}				
In			0.21 ± 0.09 g m^{-2} d^{-1}	< 80			
Cu			0.16 ± 0.15 g m^{-2} d^{-1}	< 42			
Ti			0.07 ± 0.02 g m^{-2} d^{-1}	< 40			
Ni/Fe deposition *in situ*	CH_4	Enriched mixed culture	2,600 mL L^{-1} d^{-1}	90-94	-1.50 V	-64 A m^{-2}	[91]
Electroless-Cu	CH_4	Enriched mixed culture	3.22 g m^{-3} d^{-1}	/	-0.87 V	-0.6 A m^{-2}	[95]
CC with gold NPs	Acetate	*S. ovata*	10.87 ± 2.64 g m^{-2} d^{-1}	83 ± 14	-0.37 V	-0.39 ± 0.043 A m^{-2}	[55]
CC with palladium NPs			8.47 ± 2.10 g m^{-2} d^{-1}	79 ± 16		-0.32 ± 0.064 A m^{-2}	
CC with nickel NPs			8.17 ± 1.98 g m^{-2} d^{-1}	80 ± 15		-0.30 ± 0.048 A m^{-2}	
Porous hollow fiber nickel	CH_4	Enriched mixed culture	140 ± 13 mmol m^{-2} d^{-1}	77.5 ± 3.0	-0.77 V	-1.3 ± 0.1 A m^{-2}	[22]
Porous nickel hollow fibers with CNTs modified	Acetate	*S. ovata*	1.85 ± 0.13 g m^{-2} d^{-1}	75 ± 5	-0.37 V	-0.332 ± 0.024 A m^{-2}	[101]
Porous nickel hollow fibers			1.09 ± 0.03 g m^{-2} d^{-1}	83 ± 8		-0.214 ± 0.015 A m^{-2}	
Electroless nickel plating on CHF	Acetate	Enriched mixed culture	71.72 ± 4.33 g m^{-2} d^{-1}	32.8	-0.87 V	-9.2 ± 0.7 A m^{-2}	[102]
	CH_4		6.9 ± 3.1 mM	25.4			

Hollow fiber wrapped with Ni-foam/CNTs	Acetate	Enriched mixed culture	2.82 ± 1.10 g m^{-2} d^{-1}	> 90	-0.57 V	-2.8 ± 0.2 A m^{-2}	[103]
	CH_4		240.0 ± 32.2 mmol m^{-2} d^{-1}				
Tin	CH_4	*M. maripaludis*	10 mmol L^{-1} d^{-1}	> 90	-1.17 V	-26.6 A m^{-2}	[107]
Sn-modified CF	Acetate	Enriched mixed culture	0.32 g L^{-1} d^{-1}	/	-1.07 V	-8.4 ± 1.0 A m^{-2}	[24]
Alloys and inorganic metal compound catalysts							
Fe(III) oxide-graphitized carbon nanostructures	Acetate	*S. ovata*	1.49 × 10^4 g m^{-3} d^{-1}	86 ± 9	-0.67 V	/	[109]
$NiFe_2O_4$@CF	Butyrate	Enriched mixed culture	0.19 g L^{-1} d^{-1}	/	-0.57 V	-0.14 A m^{-2}	[110]
Copper ferrite/rGO	VFA	Enriched mixed culture	35.37 g^{-1} m^{-2} d^{-1}	77.8	-0.54 V	-7.3 A m^{-2}	[112]
MXene@CF	Acetic acid	Enriched mixed culture	51 mg L^{-1} d^{-1}	41	-0.57 V	-0.17 A m^{-2}	[117]
	Butyric acid		58.13 mg L^{-1} d^{-1}				
	Propionic acid		104.53 mg L^{-1} d^{-1}				
CNT-MXene@Sponge	Butyrate	Enriched mixed culture	-0.156 g L^{-1} d^{-1}	20		-0.324 A m^{-2}	[118]
Mo_2C	Acetate	Enriched mixed culture	0.19 ± 0.02 g L^{-1} d^{-1}	64 ± 0.7	-0.57 V	-127.8 A m^{-2}	[123]
MoS_2	Acetate	Enriched mixed culture	0.2 g L^{-1} d^{-1}	58.1	-0.85 V	-14 mA	[125]
Cobalt phthalocyanine	Acetate	*C. ljungdahlii*	0.51 g L^{-1} d^{-1}	/	-0.82 V	-49 mA	[126]
	Ethanol		0.12 g L^{-1} d^{-1}		-1.57 V		
Composite materials							
rGO-CuF	Acetate	*S. ovata*	101.94 ± 17.9 g m^{-2} d^{-1}	70.2 ± 14.1	-0.99 V	-21.6 ± 2.1 A m^{-2}	[129]
Stainless steel/GF	Acetate	*C. ljungdahlii*	0.14 g L^{-1} d^{-1}	89.2	-0.87 V	-10 A m^{-2}	[130]
		Enriched mixed culture	0.078 g L^{-1} d^{-1}	49.9			
CC/stainless steel	VFA	Enriched mixed culture	1.4 g L^{-1}	/	-0.20 V	-1.13 mA	[131]
Stainless steel/GAC	Acetate	Enriched mixed culture	0.16 g L^{-1} d^{-1}	55	-0.85 V	-4.7 A m^{-2}	[132]
A porous hollow stainless steel/graphene foam	CH_4	Enriched mixed culture	848.0 ± 124.5 mmol m^{-2} d^{-1}	84.2 ± 7.7	-0.77 V	-9.7 A m^{-2}	[133]
Nano-titanium carburizing electrode	Acetate	Enriched mixed culture	11.7 mg L^{-1} d^{-1}	/	-0.57 V	-2.75 ± 0.2 A m^{-2}	[134]
	Butyrate		4.3 mg L^{-1} d^{-1}				
Fe_3O_4/GAC	Acetate	Enriched mixed culture	0.171 g L^{-1} d^{-1}	73.1	-0.82 V	-12.6 mA	[136]
rGO/Fe_3O_4 scaffold	CH_4	MEC reactor effluent	605 ± 119 mmol m^{-2} d^{-1}	91.5	-0.67 V	-6.8 A m^{-2}	[137]
MnO_2/rGO nanohybrids	VFA	MES reactor effluent	50.07 g m^{-2} d^{-1}	66.4	-0.52 V	-23.4 mA	[139]
rGO/WO_3 nanofibrous	Acetate	Enriched mixed culture	0.16 g L^{-1} d^{-1}	72	-0.50 V	-13.56 ± 0.5 A m^{-2}	[140]

into multicarbon products through their own metabolic mechanisms, corresponding to the dark reaction[145].

Liu *et al.* initially introduced the artificial photosynthesis strategy in MES, aiming to emulate the inherent mechanisms of the natural photosynthetic process[146]. This process involves two steps: first, light is captured by a highly biocompatible silicon (Si) nanowire cathode, resulting in the generation of reducing equivalents on the cathode; second, *S. ovata* biocatalysts are directly interfaced with the Si nanowire and utilize the reducing equivalents for the targeted synthesis of multicarbon products via CO_2 fixation [Figure 5A-D]. By coupling solar energy with non-photosynthetic microbial systems, a significant acetate production yield of 6 g L^{-1} was achieved. To address the adverse alkaline local environment caused by high overpotential in the MES system, a tightly packed Si nanowire-bacteria cathode was constructed by adjusting the bulk electrolyte pH and enhancing its buffering capacity[147]. What is certainly encouraging is that this approach resulted in a higher conversion efficiency from solar energy to acetate due to increased microorganism loading and improved cathode-bacteria integration. Additionally, to leverage the photoactivity of Si, an n^+/p-Si electrode was utilized in conjunction with a Ni-Mo alloy as the cathode[148]. The H_2 produced from the photocathode was then utilized by *Methanosarcina barkeri* for CO_2 reduction, resulting in CH_4 production with a FE of 82% ± 10% and a low overpotential of 175 mV. Furthermore, by replacing the n^+/p-Si photocathode with a platinum-coated p-InP cathode, the microbial photoelectrochemical system achieved fully unassisted solar-to-CH_4 conversion.

To enhance and diversify the functionality of single photocatalysts, additional functional nanomaterials were incorporated. Titanium dioxide (TiO_2), widely recognized for its photostability, abundance, low cost, and biocompatibility, has limitations due to its large band gap (3.2 eV for anatase and 3.0 eV for the rutile phase), which restricts its activation to UV light irradiation[149]. Moreover, rapid recombination of photogenerated electron-hole pairs in TiO_2 hinders the efficiency and selectivity of CO_2 reduction[150]. To address these challenges, two materials, silicon dioxide (SiO_2) porous materials and rGO nanosheets, were introduced to enhance their effectiveness in the visible spectrum and facilitate photo-induced charge-carrier separation, respectively[151]. The resulting rGO-SiO_2-TiO_2 nanocomposite was developed as a photoelectrochemical cathode for the electroreduction of CO_2, demonstrating acetate production of 0.1926 g L^{-1} d^{-1} with a coulombic Efficiency of acetate 78% and a current density 2.7 A m^{-2}.

Heterojunction photocatalyst

Despite the proposals of various strategies to modify single semiconductors, the efficient separation of photogenerated electron-hole pairs remains a highly challenging task, leading to unsatisfactory solar-to-chemical conversion efficiencies[152]. One promising approach to address this challenge is the engineering of heterojunctions in photocatalysts, encompassing both conventional heterojunctions and Z-scheme heterojunctions. These approaches can effectively modulate the energy level structure to facilitate electron-hole pair separation[153-155].

Recently, conventional heterojunctions have been employed as cathode materials in MES systems. For instance, the type I semiconductor heterostructure CuO/g-C_3N_4 was introduced as a cathode material due to its favorable photo-induced charge-carrier separation and light absorption properties[156]. Furthermore, the biocatalytic activity was enhanced by increasing the total amount of mixed culture and regulating its composition. This led to a notable acetate production rate of 0.16 g L^{-1} d^{-1} for the CuO/g-C_3N_4 photocathode. To further enhance the photocatalytic activity and stability, rGO was incorporated into the photocathodes to mitigate the recombination rate of photogenerated carriers. Combining this enhancement with the factors for improved electrocatalytic activity, the acetate production of the MES system using the

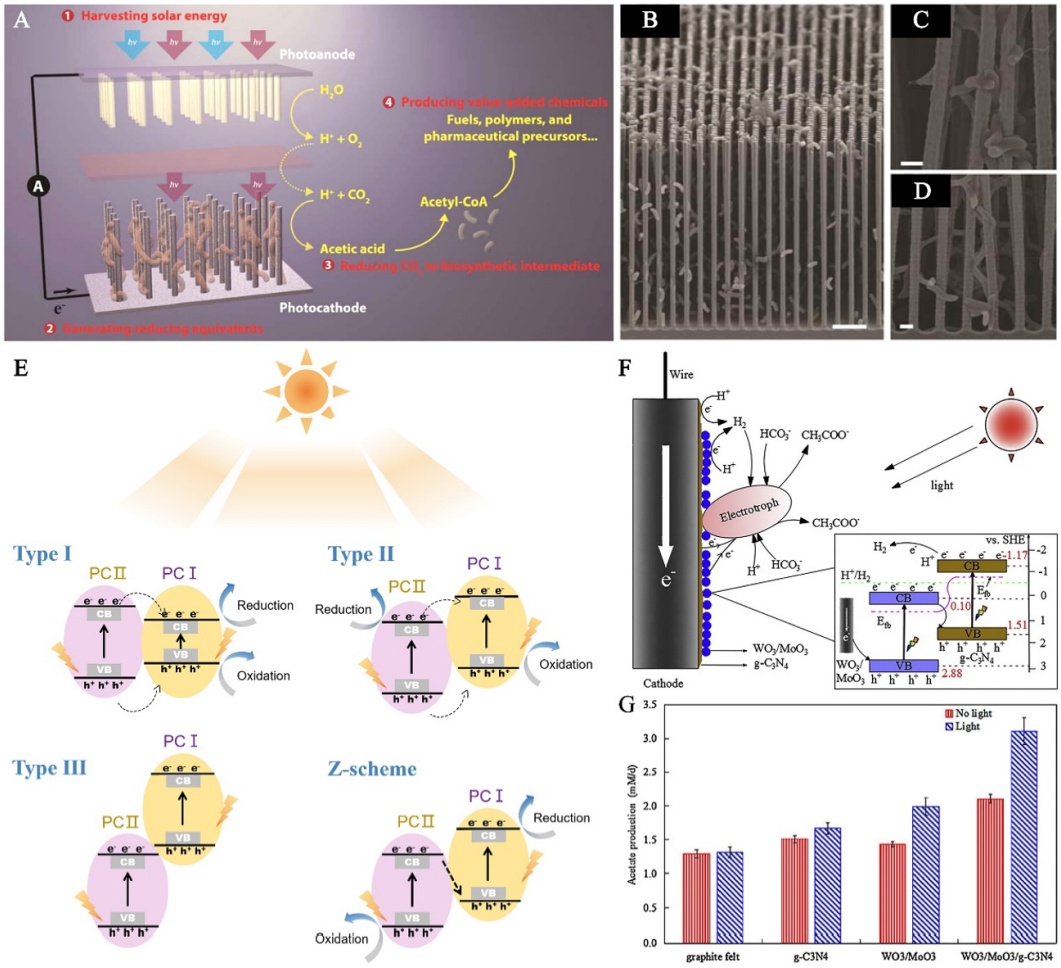

Figure 5. (A) Schematic of the microbial photoelectrochemical system with a Si nanowire array. The proposed approach for solar-powered CO_2 fixation includes four general components: (1) harvesting solar energy, (2) generating reducing equivalents, (3) reducing CO_2 to biosynthetic intermediates, and (4) producing value-added chemicals. (B) Cross-sectional SEM image of the cathode integrating the Si nanowire arrays with the microorganisms. Magnified image of (C) the middle and (D) bottom regions of the Si nanowire arrays. Scale bars: (B) 5 μm and (C and D) 1 μm. (E) Heterojunction mechanism of type I, type II, type III, and Z-scheme heterojunctions. (F) Schematic diagram of the $WO_3/MoO_3/g\text{-}C_3N_4$ photocathode in the photocatalyst-assisted MES system. (G) Comparison of acetate production of the $WO_3/MoO_3/g\text{-}C_3N_4$ photocathode in the presence or absence of light (operational time: 12 h). This figure is quoted with permission from Liu *et al.*[146] and Cai *et al.*[162].

$CuO/g\text{-}C_3N_4/rGO$ photocathode successfully increased to 0.27 g L^{-1} d^{-1}[157]. However, despite the improved photocatalytic performance of conventional heterojunctions, their electron transfer mechanism fundamentally falls short when compared to Z-scheme semiconductor heterojunctions.

The electron transfer pathway in Z-scheme heterojunctions resembles a "Z" shape, closely resembling the electron transfer chain of the light reaction in natural photosynthesis. In light reaction, the photosystem II (PS II) and photosystem I (PS I) collectively form an electron transfer chain known as the "Z-scheme" due to the "Z" shape arrangement of electron transfer entities based on their redox potentials[158-160]. Z-scheme heterojunctions allow for efficient photoelectrochemical processes within a single electrode, which utilizes two heterogeneous semiconductors to produce photogenerated electrons with higher reducibility and holes with higher oxidizability compared to the conventional electron transfer mechanisms (types I, II, and III; shown in Figure 5E)[152,161]. The most exemplary material used to construct Z-scheme heterojunctions for

optimizing MES photocathodes is graphitic-like nitrogen carbide (g-C_3N_4), owing to its excellent reduction properties with a conduction band edge position of -1.2 eV (*vs.* SHE), visible-light responsivity with a band gap of 2.68 eV, low cost, and high stability[162-164]. However, the performance of g-C_3N_4 is not optimal because photogenerated electrons and holes can recombine easily. One way to overcome this problem is to combine g-C_3N_4 with narrow-band gap semiconductors, such as WO_3/MoO_3 with a band gap of 2.77 eV, to form Z-scheme heterojunctions[162,163,165]. When coupled with g-C_3N_4 and WO_3/MoO_3, the high biocompatibility WO_3/MoO_3/g-C_3N_4 photocathode provided conductive band electrons directly or indirectly to the adhesive *Serratia marcescens* Q1, generating acetate from HCO_3^- at a rate of 0.187 g L^{-1} d^{-1} successfully [Figure 5F and G][162].

To evaluate the potential of this new type of cathode material for simultaneous removal of heavy metal Cr(VI) ions and acetate generation, $K_2Cr_2O_7$ was added to the catholyte as a simulation of industrial wastewater[163]. Compared with WO_3/MoO_3, Ag_3PO_4 owns a narrower band gap of 2.36 eV but suffers a common threat of photo-corrosion[164]. Therefore, a strategy of H_2O_2 *in-situ* generation on Ag_3PO_4/g-C_3N_4 cathodes was proposed to suppress photo-corrosion effectively and capable of producing acetate at a higher rate of 0.25 g L^{-1} d^{-1} by forming biohybrid with *S. marcescens* Q1[164]. By analogy, it is reasonable that when combining g-C_3N_4 with α-Fe_2O_3, which has a narrower band gap than WO_3/MoO_3 and Ag_3PO_4, it shows an even higher acetate production rate of 0.33 g L^{-1}[166]. The conduction band edge of the mentioned Z-scheme heterojunctions as cathode materials is -1.2 eV (*vs.* SHE), which is not sufficient to generate high H_2 production rates, while $MnFe_2O_4$ has a more negative conduction band edge value of -1.6 eV (*vs.* SHE). Thus, it may be an ideal material for photoelectrochemical cathode modification[167]. However, the common mechanism of $MnFe_2O_4$/g-C_3N_4 is type II, which means lower efficiencies of the separating than the Z-scheme[167]. To realize the charge transfer mechanism switch from type II to Z-scheme, urea treatment has been provided as a reference method[168,169]. The urea-treated $MnFe_2O_4$/g-C_3N_4 photocathode incorporating *S. marcescens* obtains the highest acetate production of 0.51 ± 0.036 g L^{-1} d^{-1} and a CE of 96% ± 3%.

The aforementioned findings validate that photocatalyst-assisted MES systems, utilizing solar energy as an electron source, offer a viable and effective artificial photosynthetic strategy for low-energy CO_2 fixation and sustainable production of value-added chemicals. The specific data of photocatalyst-assisted MES systems mentioned in this section are summarized in Table 2 below. From Table 2, it can be seen that several studies have explored the combination of single photocatalysts, such as Si, InP, or TiO_2, with biocatalysts as MES photocathodes to achieve solar-to-chemical conversion. However, single photocatalysts often suffer from the easy recombination of electron-hole pairs. These single photocatalysts had a maximum CE or FE value of only 78%, and the specific rates of acetic acid production were vague and unsatisfactory. In contrast, heterojunction photocatalysts exhibit greater potential for photochemical conversion due to their superior energy level structure. Traditional semiconductor heterostructures, such as type I semiconductor heterostructures, struggle to achieve the same degree of electron-hole separation as Z-scheme heterojunctions. Thus, Z-scheme heterojunctions achieves the highest acetate production of 0.51 ± 0.036 g L^{-1} d^{-1} and the highest CE of 96% ± 3% to date.

PERSPECTIVES AND REMAINING CHALLENGES

Despite the fact that rapid breakthroughs have been achieved in the field of MES in the past decade, several key aspects related to the development and commercialization of MES technology still need to be addressed. Looking ahead, we recommend directing future research attention towards the following aspects.

(1) Enhance the interface interaction between cathode materials and EAMs. Current cathode research primarily focuses on improving electrode surface properties[28,170] and cultivating pure bacterial biofilms[171].

Table 2. Performance of different types of cathode materials in photocatalyst-MES systems

Cathode materials	Type of photocatalyst	Type of products	Microbial inoculum	Production rate	CE or FE (%)	Cathode potential (*vs.* SHE)	Current density (A m^{-2})	Ref.
Si NW	Single	Acetate	*S. ovata*	6 g L^{-1}	/	-0.21 V	-3.5	[146]
p-InP	Single	CH_4	*M. barkeri*	22.9 nmol d^{-1}	74	/	-0.57	[148]
rGO-SiO_2-TiO_2	Single	Acetate	Enriched mixed culture	0.19 g L^{-1} d^{-1}	78	-0.77 V	-2.7	[151]
CuO/g-C_3N_4	Conventional type I	Acetate	Enriched mixed culture	0.16 g L^{-1} d^{-1}	/	-0.82 V	-114	[156]
CuO/g-C_3N_4/rGO	Conventional type I	Acetate	Enriched mixed culture	0.27 g L^{-1} d^{-1}	/	-0.67 V	-14.8	[157]
Ag_3PO_4/g-C_3N_4	Z-scheme	Acetate	*S. marcescens* Q1	0.324 ± 0.006 g L^{-1} d^{-1}	93 ± 2	1.10 V	-3.3	[164]
α-Fe_2O_3/g-C_3N_4	Z-scheme	Acetate	Enriched mixed culture	0.33 g L^{-1} d^{-1}		-0.67 V	-13.5	[166]
$MnFe_2O_4$/g-C_3N_4	Type II to Z-scheme	Acetate	*S. marcescens* Q1	0.51 ± 0.036 g L^{-1} d^{-1}	96	-1.10 V	-5.1 ± 0.2	[167]

However, the high resistance of the bacteria themselves hinders EET to some extent. By incorporating nanomaterials with enhanced biocompatibility, conductivity, and catalytic activity to modify the surface of individual bacteria, stronger interactions between each bacterium and the cathode material can be facilitated.

(2) Investigate the mechanism of electron transfer in EAMs. While significant progress has been made in understanding the electron transfer mechanism of exoelectrogens in MFCs[172-174], our understanding of EAMs in MES is still limited. A comprehensive understanding of the molecular mechanism underlying electron transfer between cathode materials and microbial cells is crucial for the development of strategies to enhance MES. To address this knowledge gap and advance MES research, advanced *in situ* analysis methods or instruments are needed to accurately capture information at the single-cell or even single-molecule level.

(3) Employ genetic engineering transformations. Genetic editing techniques can be used to fundamentally regulate the expression of proteins or enzymes associated with extracellular electron intake and intracellular anabolism[175,176]. This approach can effectively enhance the biocatalytic activity of EAMs, leading to improved MES performance.

(4) Expand the existing reactor scale. Currently, the range of value-added products for MES has expanded from gaseous products (such as methane) and short carbon-chain organic compounds (such as acetic acids) to long carbon compounds (such as caprylic acids) and alcohols (such as ethanol, isopropanol, and n-butanol). However, the reactors are mostly limited to the laboratory scale, as most of the studies mentioned in our manuscript. If the technological readiness level (TRL) is adopted to assess MES technology, it is catching up with TRL 4 and 5, which means that it is under technological validation and demonstration in relevant environments. To achieve a larger scale and a higher TRL level, not only the electrodes need to be developed, but all factors influencing the MES

system, such as temperature[71,177], medium[178], reactor construction[179,180], *etc*., need to be comprehensively taken into account.

CONCLUSION

MES is a sustainable and environmentally friendly technology capable of converting CO_2 into value-added chemicals through the integration of renewable electricity with microbial metabolism, thereby playing a crucial role in mitigating CO_2 emissions. However, the application of MES is still constrained by the limited yield of value-added chemicals, which is closely linked to the performance of cathode materials. This review provides a comprehensive overview of the research progress and performance outcomes of various cathode materials since the inception of the MES concept. Based on the different sources of electrons and the types of cathode materials, the review is organized into two main sections: cathode materials in electrocatalyst-assisted and photocatalyst-assisted MES systems. In each section, based on the type of electrode materials, we then elaborate on the effects of metal-free materials, metal materials, composite materials, single photocatalysts, and heterojunction photocatalysts on the MES system.

On the whole, for electrocatalyst-assisted microbial electrolysis systems, when considering the electrode costs, carbonaceous materials are undoubtedly the most inexpensive and environmentally friendly cathode materials. The incorporation of conductive polymers further enhances the hydrophilicity and biocompatibility of cathodes, rendering them more suitable for the growth of microbial biofilms. Metal materials can provide higher conductivity and electrocatalytic activity, effectively promoting the direct and indirect electron transfer of electroactive bacteria. Over the years, the combination of metal-free and metal materials has emerged as a major focus in cathode research, as it allows for the integration of various material advantages and compensates for their respective shortcomings. For photocatalyst-assisted microbial electrolysis systems, heterojunction photocatalysts have received more attention compared to single photocatalysts due to their superior energy level structure, which exhibits greater potential for photochemical conversion.

In addition, we found that cathodes in MES systems have a tendency from 2D to 3D electrodes to allow more microbial colonization. However, as biofilms thicken, limitations arise in terms of biomass diffusion and EET efficiency. This challenge can be addressed by introducing highly conductive materials or coupling electrocatalytic CO_2 reduction with MES to facilitate direct or indirect electron transfer. Furthermore, the liquid phase environment of MES systems can impede gas diffusion, necessitating the development of traditional gas bubbles to GDE configurations to enhance the effective transfer of CO_2 and biomass. These findings shed light on the potential strategies to improve the yield of value-added chemicals and address the challenges associated with diffusion and EET efficiency, contributing to the further development and optimization of MES technology. Hence, the optimal cathode materials should be determined according to the composite factors, such as biocatalyst type, reactor configuration, electrolyte characteristics, and more, in the actual MES system.

DECLARATIONS

Authors' contributions

Proposed the topic of this review: Hui S, Jiang Y
Performed literature survey and prepared the manuscript: Hui S, Jiang Y
Collectively discussed and revised the manuscript: Hui S, Jiang Y
Review, conceptualization, and supervision: Zhu JJ, Zhu W, Lyu Z, Ding S, Song B

Availability of data and materials
Not applicable.

Financial support and sponsorship
This work was supported by the National Natural Science Foundation of China grant 22174061, the Natural Science Foundation of Jiangsu Province grant BK20210189, the Fundamental Research Funds for the Central Universities (021114380183, 021114380189), and the Research Funds from Frontiers Science Center for Critical Earth Material Cycling of Nanjing University.

Conflicts of interest
All authors declared that there are no conflicts of interest.

Ethical approval and consent to participate
Not applicable.

Consent for publication
Not applicable.

REFERENCES
1. Liao JC, Mi L, Pontrelli S, Luo S. Fuelling the future: microbial engineering for the production of sustainable biofuels. *Nat Rev Microbiol* 2016;14:288-304. DOI PubMed
2. Davis SJ, Caldeira K, Matthews HD. Future CO_2 emissions and climate change from existing energy infrastructure. *Science* 2010;329:1330-3. DOI PubMed
3. Turner JM. The matter of a clean energy future. *Science* 2022;376:1361. DOI
4. Fu J, Li P, Lin Y, et al. Fight for carbon neutrality with state-of-the-art negative carbon emission technologies. *Eco-Environ Health* 2022;1:259-79. DOI
5. Nevin KP, Woodard TL, Franks AE, Summers ZM, Lovley DR. Microbial electrosynthesis: feeding microbes electricity to convert carbon dioxide and water to multicarbon extracellular organic compounds. *mBio* 2010;1:e00103-10. DOI PubMed PMC
6. Prévoteau A, Carvajal-Arroyo JM, Ganigué R, Rabaey K. Microbial electrosynthesis from CO_2: forever a promise? *Curr Opin Biotechnol* 2020;62:48-57. DOI PubMed
7. Rabaey K, Rozendal RA. Microbial electrosynthesis - revisiting the electrical route for microbial production. *Nat Rev Microbiol* 2010;8:706-16. DOI PubMed
8. Wang R, Li H, Sun J, et al. Nanomaterials facilitating microbial extracellular electron transfer at interfaces. *Adv Mater* 2021;33:e2004051. DOI
9. Tan X, Nielsen J. The integration of bio-catalysis and electrocatalysis to produce fuels and chemicals from carbon dioxide. *Chem Soc Rev* 2022;51:4763-85. DOI PubMed
10. Zeng AP. New bioproduction systems for chemicals and fuels: needs and new development. *Biotechnol Adv* 2019;37:508-18. DOI PubMed
11. Jourdin L, Burdyny T. Microbial electrosynthesis: where do we go from here? *Trends Biotechnol* 2021;39:359-69. DOI PubMed
12. LaBelle EV, Marshall CW, May HD. Microbiome for the electrosynthesis of chemicals from carbon dioxide. *ACC Chem Res* 2020;53:62-71. DOI PubMed
13. Jiang Y, Tian S, Li H, Xia A, Song B, Zhu W. Harnessing microbial electrosynthesis for a sustainable future. *Innov Mater* 2023;1:100008. DOI
14. Borole AP, Reguera G, Ringeisen B, Wang ZW, Feng Y, Kim BH. Electroactive biofilms: current status and future research needs. *Energy Environ Sci* 2011;4:4813-34. DOI
15. Chatterjee P, Dessì P, Kokko M, Lakaniemi A, Lens P. Selective enrichment of biocatalysts for bioelectrochemical systems: a critical review. *Renew Sustain Energy Rev* 2019;109:10-23. DOI
16. Bajracharya S, Krige A, Matsakas L, Rova U, Christakopoulos P. Advances in cathode designs and reactor configurations of microbial electrosynthesis systems to facilitate gas electro-fermentation. *Bioresour Technol* 2022;354:127178. DOI PubMed
17. Aryal N, Ammam F, Patil SA, Pant D. An overview of cathode materials for microbial electrosynthesis of chemicals from carbon dioxide. *Green Chem* 2017;19:5748-60. DOI

18. Bian B, Bajracharya S, Xu J, Pant D, Saikaly PE. Microbial electrosynthesis from CO_2: challenges, opportunities and perspectives in the context of circular bioeconomy. *Bioresour Technol* 2020;302:122863. DOI PubMed
19. Jourdin L, Freguia S, Donose BC, et al. A novel carbon nanotube modified scaffold as an efficient biocathode material for improved microbial electrosynthesis. *J Mater Chem A* 2014;2:13093-102. DOI
20. Wu B, Lin R, Kang X, Deng C, Dobson AD, Murphy JD. Improved robustness of ex-situ biological methanation for electro-fuel production through the addition of graphene. *Renew Sustain Energy Rev* 2021;152:111690. DOI
21. He Y, Li J, Zhang L, et al. 3D-printed GA/PPy aerogel biocathode enables efficient methane production in microbial electrosynthesis. *Chem Eng J* 2023;459:141523. DOI
22. Alqahtani MF, Katuri KP, Bajracharya S, Yu Y, Lai Z, Saikaly PE. Porous hollow fiber nickel electrodes for effective supply and reduction of carbon dioxide to methane through microbial electrosynthesis. *Adv Funct Mater* 2018;28:1804860. DOI
23. Zhu X, Jack J, Bian Y, Chen X, Tsesmetzis N, Ren ZJ. Electrocatalytic membranes for tunable syngas production and high-efficiency delivery to biocompatible electrolytes. *ACS Sustain Chem Eng* 2021;9:6012-22. DOI
24. Qiu Z, Zhang K, Li XL, Song T, Xie J. Sn promotes formate production to enhance microbial electrosynthesis of acetate via indirect electron transport. *Bio-Chem Eng J* 2023;192:108842. DOI
25. Liu X, Dai L. Carbon-based metal-free catalysts. *Nat Rev Mater* 2016;1:16064. DOI
26. Zhao Y, Nakamura R, Kamiya K, Nakanishi S, Hashimoto K. Nitrogen-doped carbon nanomaterials as non-metal electrocatalysts for water oxidation. *Nat Commun* 2013;4:2390. DOI PubMed
27. Liu J, Liu Y, Liu N, et al. Metal-free efficient photocatalyst for stable visible water splitting via a two-electron pathway. *Science* 2015;347:970-4. DOI
28. Lekshmi GS, Bazaka K, Ramakrishna S, Kumaravel V. Microbial electrosynthesis: carbonaceous electrode materials for CO_2 conversion. *Mater Horiz* 2023;10:292-312. DOI PubMed
29. Wickramaarachchi K, Minakshi M, Aravindh SA, et al. Repurposing N-doped grape marc for the fabrication of supercapacitors with theoretical and machine learning models. *Nanomaterials* 2022;12:1847. DOI PubMed PMC
30. Yuan Y, Liu T, Fu P, Tang J, Zhou S. Conversion of sewage sludge into high-performance bifunctional electrode materials for microbial energy harvesting. *J Mater Chem A* 2015;3:8475-82. DOI
31. You PY, Kamarudin SK. Recent progress of carbonaceous materials in fuel cell applications: an overview. *Chem Eng J* 2017;309:489-502. DOI
32. Li S, Cheng C, Thomas A. Carbon-based microbial-fuel-cell electrodes: from conductive supports to active catalysts. *Adv Mater* 2017;29:1602547. DOI
33. Kadier A, Kalil MS, Abdeshahian P, et al. Recent advances and emerging challenges in microbial electrolysis cells (MECs) for microbial production of hydrogen and value-added chemicals. *Renew Sustain Energy Rev* 2016;61:501-25. DOI
34. Zhen G, Lu X, Kumar G, Bakonyi P, Xu K, Zhao Y. Microbial electrolysis cell platform for simultaneous waste biorefinery and clean electrofuels generation: Current situation, challenges and future perspectives. *Prog Energy Combust Sci* 2017;63:119-45. DOI
35. Cheng S, Xing D, Call DF, Logan BE. Direct biological conversion of electrical current into methane by electromethanogenesis. *Environ Sci Technol* 2009;43:3953-8. DOI PubMed
36. Ni J, Li Y. Carbon nanomaterials in different dimensions for electrochemical energy storage. *Adv Energy Mater* 2016;6:1600278. DOI
37. Jin H, Guo C, Liu X, et al. Emerging two-dimensional nanomaterials for electrocatalysis. *Chem Rev* 2018;118:6337-408. DOI
38. Marshall CW, Ross DE, Fichot EB, Norman RS, May HD. Long-term operation of microbial electrosynthesis systems improves acetate production by autotrophic microbiomes. *Environ Sci Technol* 2013;47:6023-9. DOI PubMed
39. Villano M, Scardala S, Aulenta F, Majone M. Carbon and nitrogen removal and enhanced methane production in a microbial electrolysis cell. *Bioresour Technol* 2013;130:366-71. DOI
40. Dong Z, Wang H, Tian S, et al. Fluidized granular activated carbon electrode for efficient microbial electrosynthesis of acetate from carbon dioxide. *Bioresour Technol* 2018;269:203-9. DOI
41. Fan Q, Su J, Sun T, et al. Advances of the functionalized carbon nitrides for electrocatalysis. *Carbon Energy* 2022;4:211-36. DOI
42. Shakeel S, Anwer AH, Khan MZ. Nitric acid treated graphite granular cathode for microbial electro reduction of carbon dioxide to acetate. *J Cleaner Prod* 2020;269:122391. DOI
43. Chen LF, Yu H, Zhang J, Qin HY. A short review of graphene in the microbial electrosynthesis of biochemicals from carbon dioxide. *RSC Adv* 2022;12:22770-82. DOI PubMed PMC
44. Qiu HJ, Guan Y, Luo P, Wang Y. Recent advance in fabricating monolithic 3D porous graphene and their applications in biosensing and biofuel cells. *Biosens Bioelectron* 2017;89:85-95. DOI PubMed
45. Strübing D, Moeller AB, Mößnang B, Lebuhn M, Drewes JE, Koch K. Anaerobic thermophilic trickle bed reactor as a promising technology for flexible and demand-oriented H_2/CO_2 biomethanation. *Appl Energy* 2018;232:543-54. DOI
46. Deutzmann JS, Kracke F, Gu W, Spormann AM. Microbial electrosynthesis of acetate powered by intermittent electricity. *Environ Sci Technol* 2022;56:16073-81. DOI PubMed
47. Guo S, Garaj S, Bianco A, Ménard-moyon C. Controlling covalent chemistry on graphene oxide. *Nat Rev Phys* 2022;4:247-62. DOI
48. Wu J, Lin H, Moss DJ, Loh KP, Jia B. Graphene oxide for photonics, electronics and optoelectronics. *Nat Rev Chem* 2023;7:162-83. DOI
49. Lin T, Ding W, Sun L, Wang L, Liu CG, Song H. Engineered shewanella oneidensis-reduced graphene oxide biohybrid with enhanced

biosynthesis and transport of flavins enabled a highest bioelectricity output in microbial fuel cells. *Nano Energy* 2018;50:639-48. DOI

50. Yong YC, Yu YY, Zhang X, Song H. Highly active bidirectional electron transfer by a self-assembled electroactive reduced-graphene-oxide-hybridized biofilm. *Angew Chem Int Ed* 2014;53:4480-3. DOI
51. Choi S, Kim C, Suh JM, Jang HW. Reduced graphene oxide-based materials for electrochemical energy conversion reactions. *Carbon Energy* 2019;1:85-108. DOI
52. Song TS, Zhang H, Liu H, et al. High efficiency microbial electrosynthesis of acetate from carbon dioxide by a self-assembled electroactive biofilm. *Bioresour Technol* 2017;243:573-82. DOI
53. Chen L, Tremblay PL, Mohanty S, Xu K, Zhang T. Electrosynthesis of acetate from CO_2 by a highly structured biofilm assembled with reduced graphene oxide-tetraethylene pentamine. *J Mater Chem A* 2016;4:8395-401. DOI
54. Katuri KP, Kamireddy S, Kavanagh P, et al. Electroactive biofilms on surface functionalized anodes: the anode respiring behavior of a novel electroactive bacterium, Desulfuromonas acetexigens. *Water Res* 2020;185:116284. DOI
55. Zhang T, Nie H, Bain TS, et al. Improved cathode materials for microbial electrosynthesis. *Energy Environ Sci* 2013;6:217-24. DOI
56. Flexer V, Chen J, Donose BC, Sherrell P, Wallace GG, Keller J. The nanostructure of three-dimensional scaffolds enhances the current density of microbial bioelectrochemical systems. *Energy Environ Sci* 2013;6:1291-8. DOI
57. Flexer V, Jourdin L. Purposely designed hierarchical porous electrodes for high rate microbial electrosynthesis of acetate from carbon dioxide. *ACC Chem Res* 2020;53:311-21. DOI PubMed
58. Logan B, Cheng S, Watson V, Estadt G. Graphite fiber brush anodes for increased power production in air-cathode microbial fuel cells. *Environ Sci Technol* 2007;41:3341-6. DOI PubMed
59. Liu C, Yuan X, Gu Y, et al. Enhancement of bioelectrochemical CO_2 reduction with a carbon brush electrode via direct electron transfer. *ACS Sustain Chem Eng* 2020;8:11368-75. DOI
60. Baek G, Saikaly PE, Logan BE. Addition of a carbon fiber brush improves anaerobic digestion compared to external voltage application. *Water Res* 2021;188:116575. DOI PubMed
61. Fan X, Zhou Y, Jin X, Song RB, Li Z, Zhang Q. Carbon material-based anodes in the microbial fuel cells. *Carbon Energy* 2021;3:449-72. DOI
62. Vidales AG, Omanovic S, Li H, Hrapovic S, Tartakovsky B. Evaluation of biocathode materials for microbial electrosynthesis of methane and acetate. *Bioelectrochemistry* 2022;148:108246. DOI PubMed
63. Ameen F, Alshehri WA, Nadhari SA. Effect of electroactive biofilm formation on acetic acid production in anaerobic sludge driven microbial electrosynthesis. *ACS Sustain Chem Eng* 2020;8:311-8. DOI
64. Zhen G, Lu X, Kobayashi T, Kumar G, Xu K. Promoted electromethanosynthesis in a two-chamber microbial electrolysis cells (MECs) containing a hybrid biocathode covered with graphite felt (GF). *Chem Eng J* 2016;284:1146-55. DOI
65. Qi X, Jia X, Wang Y, et al. Development of a rapid startup method of direct electron transfer-dominant methanogenic microbial electrosynthesis. *Bioresour Technol* 2022;358:127385. DOI
66. Tian S, Yao X, Song TS, Chu Z, Xie J, Jin W. Artificial electron mediator with nanocubic architecture highly promotes microbial electrosynthesis from carbon dioxide. *ACS Sustain Chem Eng* 2020;8:6777-85. DOI
67. Aryal N, Halder A, Tremblay PL, Chi Q, Zhang T. Enhanced microbial electrosynthesis with three-dimensional graphene functionalized cathodes fabricated via solvothermal synthesis. *Electrochim Acta* 2016;217:117-22. DOI
68. Hu N, Wang L, Liao M, Liu K. Research on electrocatalytic reduction of CO_2 by microorganisms with a graphene modified carbon felt. *Int J Hydrogen Energy* 2021;46:6180-7. DOI
69. Carrillo-peña D, Mateos R, Morán A, Escapa A. Reduced graphene oxide improves the performance of a methanogenic biocathode. *Fuel* 2022;321:123957. DOI
70. Kou T, Yang Y, Yao B, Li Y. Interpenetrated bacteria-carbon nanotubes film for microbial fuel cells. *Small Methods* 2018;2:1800152. DOI
71. Yu L, Yuan Y, Tang J, Zhou S. Thermophilic moorella thermoautotrophica-immobilized cathode enhanced microbial electrosynthesis of acetate and formate from CO_2. *Bioelectrochemistry* 2017;117:23-8. DOI
72. Peng L, Nie WB, Ding J, et al. Denitrifying anaerobic methane oxidation and anammox process in a membrane aerated membrane bioreactor: kinetic evaluation and optimization. *Environ Sci Technol* 2020;54:6968-77. DOI
73. Wu Y, Li W, Wang L, et al. Enhancing the selective synthesis of butyrate in microbial electrosynthesis system by gas diffusion membrane composite biocathode. *Chemosphere* 2022;308:136088. DOI
74. Antolini E. Composite materials for polymer electrolyte membrane microbial fuel cells. *Biosens Bioelectron* 2015;69:54-70. DOI PubMed
75. Li Q, Fu Q, Kobayashi H, et al. GO/PEDOT modified biocathodes promoting CO_2 reduction to CH_4 in microbial electrosynthesis. *Sustain Energy Fuels* 2020;4:2987-97. DOI
76. Sui ZY, Han BH. Effect of surface chemistry and textural properties on carbon dioxide uptake in hydrothermally reduced graphene oxide. *Carbon* 2015;82:590-8. DOI
77. Zeng W, Tao XM, Lin S, et al. Defect-engineered reduced graphene oxide sheets with high electric conductivity and controlled thermal conductivity for soft and flexible wearable thermoelectric generators. *Nano Energy* 2018;54:163-74. DOI
78. Chen Z, Jin L, Hao W, Ren W, Cheng HM. Synthesis and applications of three-dimensional graphene network structures. *Mater Today Nano* 2019;5:100027. DOI

79. Mubarak S, Dhamodharan D, Byun HS. Recent advances in 3D printed electrode materials for electrochemical energy storage devices. *J Energy Chem* 2023;81:272-312. DOI
80. Bose A, Gardel EJ, Vidoudez C, Parra EA, Girguis PR. Electron uptake by iron-oxidizing phototrophic bacteria. *Nat Commun* 2014;5:3391. DOI PubMed
81. Li S, Kim M, Jae J, Jang M, Jeon BH, Kim JR. Solid neutral red/Nafion conductive layer on carbon felt electrode enhances acetate production from CO_2 and energy efficiency in microbial electrosynthesis system. *Bioresour Technol* 2022;363:127983. DOI
82. Jiang YJ, Hui S, Jiang LP, Zhu JJ. Functional nanomaterial-modified anodes in microbial fuel cells: advances and perspectives. *Chemistry* 2023;29:e202202002. DOI PubMed
83. Luo H, Qi J, Zhou M, et al. Enhanced electron transfer on microbial electrosynthesis biocathode by polypyrrole-coated acetogens. *Bioresour Technol* 2020;309:123322. DOI
84. Lees EW, Mowbray BAW, Parlane FGL, Berlinguette CP. Gas diffusion electrodes and membranes for CO_2 reduction electrolysers. *Nat Rev Mater* 2022;7:55-64. DOI
85. Bajracharya S, Vanbroekhoven K, Buisman CJ, Pant D, Strik DP. Application of gas diffusion biocathode in microbial electrosynthesis from carbon dioxide. *Environ Sci Pollut Res Int* 2016;23:22292-308. DOI PubMed
86. Dessì P, Buenaño-Vargas C, Martínez-Sosa S, et al. Microbial electrosynthesis of acetate from CO_2 in three-chamber cells with gas diffusion biocathode under moderate saline conditions. *Environ Sci Ecotechnol* 2023;16:100261. DOI PubMed PMC
87. Zhao CE, Gai P, Song R, Chen Y, Zhang J, Zhu JJ. Nanostructured material-based biofuel cells: recent advances and future prospects. *Chem Soc Rev* 2017;46:1545-64. DOI
88. Nie Y, Li L, Wei Z. Recent advancements in Pt and Pt-free catalysts for oxygen reduction reaction. *Chem Soc Rev* 2015;44:2168-201. DOI
89. Zhu Y, Zhang B. Nanocarbon-based metal-free and non-precious metal bifunctional electrocatalysts for oxygen reduction and oxygen evolution reactions. *J Energy Chem* 2021;58:610-28. DOI
90. Jiang Y, Chu N, Zhang W, et al. Zinc: a promising material for electrocatalyst-assisted microbial electrosynthesis of carboxylic acids from carbon dioxide. *Water Res* 2019;159:87-94. DOI
91. Vidales A, Bruant G, Omanovic S, Tartakovsky B. Carbon dioxide conversion to C1 - C2 compounds in a microbial electrosynthesis cell with in situ electrodeposition of nickel and iron. *Electrochim Acta* 2021;383:138349. DOI
92. Zhang Y, Li P, Zhao C, et al. Multicarbons generation factory: CuO/Ni single atoms tandem catalyst for boosting the productivity of CO_2 electrocatalysis. *Sci Bull* 2022;67:1679-87. DOI
93. Huang J, Mensi M, Oveisi E, Mantella V, Buonsanti R. Structural sensitivities in bimetallic catalysts for electrochemical CO_2 reduction revealed by Ag-Cu nanodimers. *J Am Chem Soc* 2019;141:2490-9. DOI PubMed
94. Chen C, Li Y, Yu S, et al. Cu-Ag tandem catalysts for high-rate CO_2 electrolysis toward multicarbons. *Joule* 2020;4:1688-99. DOI
95. Baek G, Shi L, Rossi R, Logan BE. Using copper-based biocathodes to improve carbon dioxide conversion efficiency into methane in microbial methanogenesis cells. *Chem Eng J* 2022;435:135076. DOI
96. Zhu X, Blanco E, Bhatti M, Borrion A. Impact of metallic nanoparticles on anaerobic digestion: a systematic review. *Sci Total Environ* 2021;757:143747. DOI PubMed
97. Gao Y, Li Z, Cai J, et al. Metal nanoparticles increased the lag period and shaped the microbial community in slurry-electrode microbial electrosynthesis. *Sci Total Environ* 2022;838:156008. DOI
98. Srikanth S, Singh D, Vanbroekhoven K, et al. Electro-biocatalytic conversion of carbon dioxide to alcohols using gas diffusion electrode. *Bioresour Technol* 2018;265:45-51. DOI
99. Kim HW, Marcus AK, Shin JH, Rittmann BE. Advanced control for photoautotrophic growth and CO_2-utilization efficiency using a membrane carbonation photobioreactor (MCPBR). *Environ Sci Technol* 2011;45:5032-8. DOI PubMed
100. Katuri KP, Werner CM, Jimenez-Sandoval RJ, et al. A novel anaerobic electrochemical membrane bioreactor (AnEMBR) with conductive hollow-fiber membrane for treatment of low-organic strength solutions. *Environ Sci Technol* 2014;48:12833-41. DOI
101. Bian B, Alqahtani MF, Katuri KP, et al. Porous nickel hollow fiber cathodes coated with CNTs for efficient microbial electrosynthesis of acetate from CO_2 using *Sporomusa ovata*. *J Mater Chem A* 2018;6:17201-11. DOI
102. Bian B, Singh Y, Rabaey K, Saikaly PE. Nickel-coated ceramic hollow fiber cathode for fast enrichment of chemolithoautotrophs and efficient reduction of CO_2 in microbial electrosynthesis. *Chem Eng J* 2022;450:138230. DOI
103. Bian B, Xu J, Katuri KP, Saikaly PE. Resistance assessment of microbial electrosynthesis for biochemical production to changes in delivery methods and CO_2 flow rates. *Bioresour Technol* 2021;319:124177. DOI PubMed
104. Asimakopoulos K, Gavala HN, Skiadas IV. Reactor systems for syngas fermentation processes: a review. *Chem Eng J* 2018;348:732-44. DOI
105. Haas T, Krause R, Weber R, Demler M, Schmid G. Technical photosynthesis involving CO_2 electrolysis and fermentation. *Nat Catal* 2018;1:32-9. DOI
106. Claassens NJ, Cotton CAR, Kopljar D, Bar-even A. Making quantitative sense of electromicrobial production. *Nat Catal* 2019;2:437-47. DOI
107. Huang Y, Hu Z. An integrated electrochemical and biochemical system for sequential reduction of CO_2 to methane. *Fuel* 2018;220:8-13. DOI
108. Yang Y, Niu S, Han D, Liu T, Wang G, Li Y. Progress in developing metal oxide nanomaterials for photoelectrochemical water splitting. *Adv Energy Mater* 2017;7:1700555. DOI

109. Cui M, Nie H, Zhang T, Lovley D, Russell TP. Three-dimensional hierarchical metal oxide-carbon electrode materials for highly efficient microbial electrosynthesis. *Sustain Energy Fuels* 2017;1:1171-6. DOI
110. Tahir K, Miran W, Jang J, Woo SH, Lee DS. Enhanced product selectivity in the microbial electrosynthesis of butyrate using a nickel ferrite-coated biocathode. *Environ Res* 2021;196:110907. DOI
111. Wang L, Bock DC, Li J, et al. Synthesis and characterization of $CuFe_2O_4$ nano/submicron wire-carbon nanotube composites as binder-free anodes for Li-ion batteries. *ACS Appl Mater Interfaces* 2018;10:8770-85. DOI
112. Thatikayala D, Min B. Copper ferrite supported reduced graphene oxide as cathode materials to enhance microbial electrosynthesis of volatile fatty acids from CO_2. *Sci Total Environ* 2021;768:144477. DOI PubMed
113. Guo Y, Du Z, Cao Z, Li B, Yang S. MXene derivatives for energy storage and conversions. *Small Methods* 2023;7:e2201559. DOI PubMed
114. Shahzad F, Alhabeb M, Hatter CB, et al. Electromagnetic interference shielding with 2D transition metal carbides (MXenes). *Science* 2016;353:1137-40. DOI
115. Zhang YZ, El-Demellawi JK, Jiang Q, et al. MXene hydrogels: fundamentals and applications. *Chem Soc Rev* 2020;49:7229-51. DOI
116. Wei Y, Zhang P, Soomro RA, Zhu Q, Xu B. Advances in the synthesis of 2D MXenes. *Adv Mater* 2021;33:e2103148. DOI
117. Tahir K, Miran W, Jang J, et al. A novel MXene-coated biocathode for enhanced microbial electrosynthesis performance. *Chem Eng J* 2020;381:122687. DOI
118. Tahir K, Maile N, Ghani AA, Kim B, Jang J, Lee DS. Development of a three-dimensional macroporous sponge biocathode coated with carbon nanotube-MXene composite for high-performance microbial electrosynthesis systems. *Bioelectrochemistry* 2022;146:108140. DOI
119. Madjarov J, Soares R, Paquete CM, Louro RO. Sporomusa ovata as catalyst for bioelectrochemical carbon dioxide reduction: a review across disciplines from microbiology to process engineering. *Front Microbiol* 2022;13:913311. DOI PubMed PMC
120. Blanchet E, Duquenne F, Rafrafi Y, Etcheverry L, Erable B, Bergel A. Importance of the hydrogen route in up-scaling electrosynthesis for microbial CO_2 reduction. *Energy Environ Sci* 2015;8:3731-44. DOI
121. Chen WF, Muckerman JT, Fujita E. Recent developments in transition metal carbides and nitrides as hydrogen evolution electrocatalysts. *Chem Commun* 2013;49:8896-909. DOI PubMed
122. Zou X, Zhang Y. Noble metal-free hydrogen evolution catalysts for water splitting. *Chem Soc Rev* 2015;44:5148-80. DOI PubMed
123. Tian S, Wang H, Dong Z, et al. Mo_2C-induced hydrogen production enhances microbial electrosynthesis of acetate from CO_2 reduction. *Biotechnol Biofuels* 2019;12:71. DOI PubMed PMC
124. Kracke F, Wong AB, Maegaard K, et al. Robust and biocompatible catalysts for efficient hydrogen-driven microbial electrosynthesis. *Commun Chem* 2019;2:45. DOI
125. Song T, Fu L, Wan N, Wu J, Xie J. Hydrothermal synthesis of MoS_2 nanoflowers for an efficient microbial electrosynthesis of acetate from CO_2. *J CO2 Util* 2020;41:101231. DOI
126. Zhu X, Jack J, Leininger A, et al. Syngas mediated microbial electrosynthesis for CO_2 to acetate conversion using clostridium ljungdahlii. *Resour Conserv Recycl* 2022;184:106395. DOI
127. Ramkumar R, Minakshi M. Fabrication of ultrathin $CoMoO_4$ nanosheets modified with chitosan and their improved performance in energy storage device. *Dalton Trans* 2015;44:6158-68. DOI PubMed
128. Hindatu Y, Annuar M, Gumel A. Mini-review: anode modification for improved performance of microbial fuel cell. *Renew Sustain Energy Rev* 2017;73:236-48. DOI
129. Aryal N, Wan L, Overgaard MH, et al. Increased carbon dioxide reduction to acetate in a microbial electrosynthesis reactor with a reduced graphene oxide-coated copper foam composite cathode. *Bioelectrochemistry* 2019;128:83-93. DOI
130. Bajracharya S, ter Heijne A, Dominguez Benetton X, et al. Carbon dioxide reduction by mixed and pure cultures in microbial electrosynthesis using an assembly of graphite felt and stainless steel as a cathode. *Bioresour Technol* 2015;195:14-24. DOI
131. Tharak A, Venkata Mohan S. Electrotrophy of biocathodes regulates microbial-electro-catalyzation of CO_2 to fatty acids in single chambered system. *Bioresour Technol* 2021;320:124272. DOI PubMed
132. Shakeel S, Khan MZ. Enhanced production and utilization of biosynthesized acetate using a packed-fluidized bed cathode based MES system. *J Environ Chem Eng* 2022;10:108067. DOI
133. Fu Q, He Y, Li Z, et al. Direct CO_2 delivery with hollow stainless steel/graphene foam electrode for enhanced methane production in microbial electrosynthesis. *Energy Convers Manag* 2022;268:116018. DOI
134. Hu N, Wang L, Liao M, Yin M. Research on the electrocatalytic reduction of CO_2 by microorganisms with a nano-titanium carburizing electrode. *Bioelectrochemistry* 2021;137:107672. DOI PubMed
135. Byrne JM, Klueglein N, Pearce C, Rosso KM, Appel E, Kappler A. Redox cycling of Fe(II) and Fe(III) in magnetite by Fe-metabolizing bacteria. *Science* 2015;347:1473-6. DOI PubMed
136. Zhu H, Dong Z, Huang Q, Song TS, Xie J. Fe_3O_4/granular activated carbon as an efficient three-dimensional electrode to enhance the microbial electrosynthesis of acetate from CO_2. *RSC Adv* 2019;9:34095-101. DOI PubMed PMC
137. He Y, Li Q, Li J, et al. Magnetic assembling GO/Fe_3O_4/microbes as hybridized biofilms for enhanced methane production in microbial electrosynthesis. *Renew Energy* 2022;185:862-70. DOI
138. Cheng J, Xia R, Li H, et al. Enhancing extracellular electron transfer of *Geobacter sulfurreducens* in bioelectrochemical systems using N-doped Fe_3O_4 @carbon dots. *ACS Sustain Chem Eng* 2022;10:3935-50. DOI
139. Thatikayala D, Pant D, Min B. MnO_2/reduced graphene oxide nanohybrids as a cathode catalyst for the microbial reduction of CO_2 to

acetate and isobutyric acid. *Sustain Energy Technol Assess* 2021;45:101114. DOI
140. Anwer AH, Khan N, Khan MD, Shahadat M, Khan MZ. High capacitive rGO/WO_3 supported nanofibers as cathode catalyst to boost-up the CO_2 sequestration via microbial electrosynthesis. *J Environ Chem Eng* 2021;9:106650. DOI
141. Barham JP, König B. Synthetic photoelectrochemistry. *Angew Chem Int Ed* 2020;59:11732-47. DOI PubMed PMC
142. Wang Q, Pan Z. Advances and challenges in developing cocatalysts for photocatalytic conversion of carbon dioxide to fuels. *Nano Res* 2022;15:10090-109. DOI
143. Fang X, Kalathil S, Reisner E. Semi-biological approaches to solar-to-chemical conversion. *Chem Soc Rev* 2020;49:4926-52. DOI PubMed
144. Nelson N, Ben-Shem A. The complex architecture of oxygenic photosynthesis. *Nat Rev Mol Cell Biol* 2004;5:971-82. DOI PubMed
145. Zhu XG, Long SP, Ort DR. Improving photosynthetic efficiency for greater yield. *Annu Rev Plant Biol* 2010;61:235-61. DOI PubMed
146. Liu C, Gallagher JJ, Sakimoto KK, et al. Nanowire-bacteria hybrids for unassisted solar carbon dioxide fixation to value-added chemicals. *Nano Lett* 2015;15:3634-9. DOI PubMed PMC
147. Su Y, Cestellos-blanco S, Kim JM, et al. Close-packed nanowire-bacteria hybrids for efficient solar-driven CO_2 fixation. *Joule* 2020;4:800-11. DOI
148. Nichols EM, Gallagher JJ, Liu C, et al. Hybrid bioinorganic approach to solar-to-chemical conversion. *Proc Natl Acad Sci USA* 2015;112:11461-6. DOI PubMed PMC
149. Zanardo D, Forghieri G, Tieuli S, et al. Effects of SiO_2-based scaffolds in TiO_2 photocatalyzed CO_2 reduction. *Catal Today* 2022;387:54-60. DOI
150. Li J, Wu N. Semiconductor-based photocatalysts and photoelectrochemical cells for solar fuel generation: a review. *Catal Sci Technol* 2015;5:1360-84. DOI
151. Anwer AH, Shoeb M, Mashkoor F, et al. Simultaneous reduction of carbon dioxide and energy harvesting using RGO-based SiO_2-TiO_2 nanocomposite for supercapacitor and microbial electrosynthesis. *Appl Catal B Environ* 2023;339:123091. DOI
152. Low J, Yu J, Jaroniec M, Wageh S, Al-Ghamdi AA. Heterojunction photocatalysts. *Adv Mater* 2017;29:1601694. DOI PubMed
153. Xie M, Fu X, Jing L, Luan P, Feng Y, Fu H. Long-lived, visible-light-excited charge carriers of TiO_2/$BiVO_4$ nanocomposites and their unexpected photoactivity for water splitting. *Adv Energy Mater* 2014;4:1300995. DOI
154. Wang M, Sun L, Lin Z, Cai J, Xie K, Lin C. *p-n* Heterojunction photoelectrodes composed of Cu_2O-loaded TiO_2 nanotube arrays with enhanced photoelectrochemical and photoelectrocatalytic activities. *Energy Environ Sci* 2013;6:1211-20. DOI
155. Yu J, Low J, Xiao W, Zhou P, Jaroniec M. Enhanced photocatalytic CO_2-reduction activity of anatase TiO_2 by coexposed {001} and {101} facets. *J Am Chem Soc* 2014;136:8839-42. DOI PubMed
156. Song TS, Li T, Tao R, Huang HF, Xie J. CuO/g-C_3N_4 heterojunction photocathode enhances the microbial electrosynthesis of acetate through CO_2 reduction. *Sci Total Environ* 2022;818:151820. DOI
157. Li T, Zhang K, Luo D, Song T, Xie J. CuO/g-C_3N_4/rGO multifunctional photocathode with simultaneous enhancement of electron transfer and substrate mass transfer facilitates microbial electrosynthesis of acetate. *Int J Hydrogen Energy* 2022;47:34875-86. DOI
158. Barber J. Photosynthetic energy conversion: natural and artificial. *Chem Soc Rev* 2009;38:185-96. DOI PubMed
159. Nozik AJ. *p-n* photoelectrolysis cells. *Appl Phys Lett* 1976;29:150-3. DOI
160. Liu C, Dasgupta NP, Yang P. Semiconductor nanowires for artificial photosynthesis. *Chem Mater* 2014;26:415-22. DOI
161. Huang D, Chen S, Zeng G, et al. Artificial Z-scheme photocatalytic system: what have been done and where to go? *Coord Chem Rev* 2019;385:44-80. DOI
162. Cai Z, Huang L, Quan X, Zhao Z, Shi Y, Li Puma G. Acetate production from inorganic carbon (HCO_3^-) in photo-assisted biocathode microbial electrosynthesis systems using WO_3/MoO_3/g-C_3N_4 heterojunctions and Serratia marcescens species. *Appl Catal B* 2020;267:118611. DOI
163. Huang L, Song S, Cai Z, Zhou P, Li Puma G. Efficient conversion of bicarbonate (HCO_3^-) to acetate and simultaneous heavy metal Cr(VI) removal in photo-assisted microbial electrosynthesis systems combining WO_3/MoO_3/g-C_3N_4 heterojunctions and Serratia marcescens electrotroph. *Chem Eng J* 2021;406:126786. DOI
164. Kong W, Huang L, Quan X, Zhao Z, Li Puma G. Efficient production of acetate from inorganic carbon (HCO_3^-) in microbial electrosynthesis systems incorporating Ag_3PO_4/g-C_3N_4 anaerobic photo-assisted biocathodes. *Appl Catal B* 2021;284:119696. DOI
165. Huang L, Xu Z, Shi Y, Zhang Y, Li Puma G. Cellular electron transfer in anaerobic photo-assisted biocathode microbial electrosynthesis systems for acetate production from inorganic carbon (HCO_3^-). *Chem Eng J* 2022;431:134022. DOI
166. Li T, Zhang K, Song T, Xie J. α-Fe_2O_3/g-C_3N_4 Z-scheme heterojunction photocathode to enhance microbial electrosynthesis of acetate from CO_2. *ACS Sustain Chem Eng* 2022;10:17308-17. DOI
167. Kong W, Huang L, Quan X, Puma GL. Synergistic induced charge transfer switch by oxygen vacancy and pyrrolic nitrogen in $MnFe_2O_4$/g-C_3N_4 heterojunctions for efficient transformation of bicarbonate to acetate in photo-assisted MES. *Appl Catal B* 2022;307:121214. DOI
168. You S, Ma M, Wang W, et al. 3D macroporous nitrogen-enriched graphitic carbon scaffold for efficient bioelectricity generation in microbial fuel cells. *Adv Energy Mater* 2017;7:1601364. DOI
169. Lau VW, Yu VW, Ehrat F, et al. Urea-modified carbon nitrides: enhancing photocatalytic hydrogen evolution by rational defect engineering. *Adv Energy Mater* 2017;7:1602251. DOI
170. Yu W, Bai H, Zeng Y, et al. Solar-driven producing of value-added chemicals with organic semiconductor-bacteria biohybrid system.

Research 2022;2022:9834093. DOI PubMed PMC

171. Vassilev I, Dessì P, Puig S, Kokko M. Cathodic biofilms - a prerequisite for microbial electrosynthesis. *Bioresour Technol* 2022;348:126788. DOI PubMed
172. Yu SS, Chen JJ, Liu XY, Yu HQ. Interfacial electron transfer from the outer membrane cytochrome OmcA to graphene oxide in a microbial fuel cell: spectral and electrochemical insights. *ACS Energy Lett* 2018;3:2449-56. DOI
173. Thapa BS, Kim T, Pandit S, et al. Overview of electroactive microorganisms and electron transfer mechanisms in microbial electrochemistry. *Bioresour Technol* 2022;347:126579. DOI
174. Xia Q, Liu R, Chen X, Chen Z, Zhu JJ. In vivo voltammetric imaging of metal nanoparticle-catalyzed single-cell electron transfer by fermi level-responsive graphene. *Research* 2023;6:0145. DOI PubMed PMC
175. Li F, Li YX, Cao YX, et al. Modular engineering to increase intracellular NAD(H/$^{+}$) promotes rate of extracellular electron transfer of Shewanella oneidensis. *Nat Commun* 2018;9:3637. DOI PubMed PMC
176. Li F, Tang R, Zhang B, et al. Systematic full-cycle engineering microbial biofilms to boost electricity production in shewanella oneidensis. *Research* 2023;6:0081. DOI PubMed PMC
177. Yang HY, Hou NN, Wang YX, et al. Mixed-culture biocathodes for acetate production from CO_2 reduction in the microbial electrosynthesis: impact of temperature. *Sci Total Environ* 2021;790:148128. DOI
178. Guo F, Babauta JT, Beyenal H. The effect of additional salinity on performance of a phosphate buffer saline buffered three-electrode bioelectrochemical system inoculated with wastewater. *Bioresour Technol* 2021;320:124291. DOI PubMed
179. Li X, Zeng C, Lu Y, Liu G, Luo H, Zhang R. Development of methanogens within cathodic biofilm in the single-chamber microbial electrolysis cell. *Bioresour Technol* 2019;274:403-9. DOI PubMed
180. Wang H, Du H, Zeng S, et al. Explore the difference between the single-chamber and dual-chamber microbial electrosynthesis for biogas production performance. *Bioelectrochemistry* 2021;138:107726. DOI